Environmental and Experimental Botany 192 (2021) 104654

Contents lists available at ScienceDirect

Environmental and Experimental Botany

journal homepage: www.elsevier.com/locate/envexpbot

Sodium uptake and transport regulation, and photosynthetic efficiency maintenance as the basis of differential salt tolerance in rice cultivars

Cibelle Gomes Gadelha [a], Ítalo Antônio Cotta Coutinho [b], Sergimar Kennedy de Paiva Pinheiro [c], Emilio de Castro Miguel [d], Humberto Henrique de Carvalho [a], Lineker de Sousa Lopes [e], Enéas Gomes-Filho [f,*]

[a] Department of Biochemistry and Molecular Biology, Science Center, Postgraduate Program in Biochemistry, Federal University of Ceará, 60440-970, Fortaleza, Ceará, Brazil
[b] Department of Biology, Science Center, Graduate Program in Systematics, Use, and Conservation of Biodiversity, Federal University of Ceará, 60440-554, Fortaleza, Ceará, Brazil
[c] Department of Metallurgical and Materials Engineering, Technology Center, Postgraduate Program in Biotechnology of Natural Resources, Federal University of Ceará, 60440-554, Fortaleza, Ceará, Brazil
[d] Department of Metallurgical and Materials Engineering, Technology Center, Postgraduate Programs in Biotechnology of Natural Resources and in Systematics, Use, and Conservation of Biodiversity, Federal University of Ceará, 60440-554, Fortaleza, Ceará, Brazil
[e] Department of Biochemistry and Molecular Biology, Science Center, Postgraduate Program in Agronomy/Phytotechnics, Federal University of Ceará, 60440-970, Fortaleza, Ceará, Brazil
[f] Department of Biochemistry and Molecular Biology, Science Center, Postgraduate Programs in Biochemistry and in Agronomy/Phytotechnics, Federal University of Ceará, Pici Campus St., 60440-970, Fortaleza, Ceará, Brazil

ARTICLE INFO

Keywords:
Salt stress
Oryza sativa
Gene expression
Photosynthesis
Ionic homeostasis
Chloroplast ultrastructure

ABSTRACT

Rice (*Oryza sativa* L.) is among the most consumed cereals in the world. Its growth is severely affected by excessive salinity, leading to considerable negative economic impacts. Thus, BRS Esmeralda and São Francisco rice cultivars, presenting antagonist cultivation recommendations and differential salt tolerance, were selected to examine how salt stress influences ionic homeostasis and photosynthetic capacity. Phenotypic, physiological, molecular, and morphological results indicated that São Francisco had a better potential to withstand salt stress than BRS Esmeralda. Although salinity promoted a significant increase in Na^+ content, particularly in BRS Esmeralda, the harmful effects were less severe in São Francisco. The upregulation of *SOS* and *NHX gene* expressions revealed that São Francisco used these mechanisms to control Na^+ accumulation in cytosol. Besides, São Francisco plants were efficient in reducing the adverse effects of salinity on photosynthesis. Under salt stress, São Francisco leaves exhibited better effective quantum efficiency of PSII, photochemical extinction coefficient, and electron transport rate. Besides, the relative energy excess in PSII and non-photochemical quenching were both smaller compared to BRS Esmeralda. Na^+ cytotoxic effects damaged the chloroplast ultrastructure in BRS Esmeralda, reducing photosynthetic capacity. In contrast, the São Francisco cultivar's better performance was followed by an efficient Na^+ exclusion and photosynthetic capacity maintenance, leading to lower growth losses. Overall, the findings are suitable for understanding salt responses and developing functional markers associated with salt stress tolerance improvement in rice.

Abbreviations: *A*, CO_2 assimilation; *A/Ci*, instantaneous carboxylation efficiency; Chl, chlorophyll; DM, dry mass; E, transpiration rate; ES, BRS Esmeralda; ETR, electron transport rate; EXC, energy excess at the PSII level; Fv/Fm, maximum quantum yield of PSII in dark-adapted leaves; g_s, stomatal conductance; NHX, Na^+/H^+ exchanger; NPQ, non-photochemical quenching; PBS, phosphate-buffered saline; PCA, principal component analysis; PPFD, photosynthetic photon flux density; qP, photochemical quenching; ROS, reactive oxygen species; SF, São Francisco; SOS, salt overly sensitive; ΦPSII, effective quantum yield of PSII.

* Corresponding author.
E-mail addresses: cibellegadelha@outlook.com.br (C.G. Gadelha), italo.coutinho@ufc.br (Í.A.C. Coutinho), sergimarkennedy@hotmail.com (S.K.P. Pinheiro), emilio.decastromiguel@gmail.com (E.C. Miguel), humberto.carvalho@ufc.br (H.H. Carvalho), linekerlk@gmail.com (L.S. Lopes), egomesf@ufc.br (E. Gomes-Filho).

https://doi.org/10.1016/j.envexpbot.2021.104654
Received 21 June 2021; Received in revised form 30 August 2021; Accepted 10 September 2021
Available online 16 September 2021

1. Introduction

Rice *(Oryza sativa* L.) is a cereal and staple food crop for more than half of the world's population (Singh et al., 2019). The importance of stimulating its production is closely related to the increasing demand for food from a growing population. However, this crop's development and grain yield is negatively affected by a range of environmental stresses (Mantri et al., 2012). Among those abiotic stresses, salinity is one of the most relevant since it affects about 1 billion hectares in more than 100 countries worldwide, thus severely compromising world agricultural productivity (FAO, 2019). The impact of salt stress on plant development is mainly due to reduced osmotic potential in the root environment and excessive Na^+ and Cl^- ions accumulation. Besides, salt stress can lead to reactive oxygen species (ROS) overproduction, disrupt regular cell metabolism, and causing damage to the cellular components (Gadelha et al., 2017).

Salt stress imposes a reduction of seed germination rate, inhibition of photosynthesis, ionic toxicity, water absorption limiting, chlorosis, and senescence, culminating in oxidative stress, reduced growth, and losses of grain yield (Singh and Sengar, 2014). Rice is considered a salt-sensitive crop (Islam et al., 2019). Then, salinity can interfere with various plant physiological functions such as water and nutritional balance, enzymatic activity, protein synthesis, and *gene* expression (Hasegawa, 2013). Remarkably, the impairment of plant growth is associated with reductions in photosynthetic rates (Mahlooji et al., 2018; Najar et al., 2019). Saline stress, in turn, causes decreased stomatal opening, limiting gas exchange, as well as damaging photosystems, electron transport, and chloroplast structure, reducing enzyme pigments and inhibiting the enzymes involved with CO_2 fixation (Negrão et al., 2017; Shahzad et al., 2019). However, not all rice varieties respond equally to salt stress. Some studies have already pointed out that some of them have distinct salinity tolerance mechanisms (Chang et al., 2019; Frukh et al., 2020; Gerona et al., 2019; Liu et al., 2019; Singh et al., 2019).

Some plants can prevent or minimize salt stress's harmful effects by reprogramming various biochemical and molecular processes. These responses are mainly related to cellular homeostasis restoration, as strict control of Na^+ accumulation in the cytosol, osmoprotectant accumulation, and antioxidant enzyme activation. Besides, there are changes in carbon metabolism, photochemistry, membrane structure modification, and plant hormones induction (Keisham et al., 2018; Shahzad et al., 2019; Wu, 2018). Strategies such as Na^+ efflux back to the growth medium or the apoplast, Na^+ compartmentalization into the vacuole, control of xylem loading, Na^+ retention in stem cells, Na^+ recirculation by phloem, the allocation of salts to old leaves, and Na^+ excretion to the leaf surface (halophytes only) are essential for salt stress tolerance (Yamaguchi et al., 2013). The ionic adjustment is mediated by channels or antiport proteins carriers (Na^+/K^+), including SOS (salt overly sensitive) and NHX (Na^+/H^+ exchanger) transporter families. The SOS signaling pathway started on the plasma membrane results in the Na^+ exclusion of the roots. Besides, NHX transporters located in the tonoplast promote the entry of Na^+ into the vacuole or endosomes (Khan et al., 2015; Wu, 2018). Both mechanisms act to maintain low levels of Na^+ cytosolic, which avoids its harmful effects on metabolism (Krishnamurthy et al., 2019).

According to EMBRAPA (2013), the São Francisco is a promissory rice cultivar since it produces 8 % more than other commercial cultivars on irrigated cultivation. Additionally, the cultivar BRS Esmeralda has high productivity in rainfed cultivation (Castro et al., 2014), and the BRS Esmeralda cultivar exhibits drought tolerance (Peres et al., 2018). However, both cultivars still needed to be tested against other abiotic stress, such as salinity. Given this, the present work aimed to broaden the knowledge about rice plants' development under saline stress and evaluate rice cultivars' differential salt tolerance, seeking to understand and elucidate the regulatory mechanisms and the molecular routes involved in this process. In our preliminary studies, the São Francisco cultivar exhibited the most tolerance compared to the other four rice cultivars, while the BRS Esmeralda cultivar was the most sensitive when grown for twelve days in the presence of 80 mM NaCl. Thereby, we hypothesized that the São Francisco cultivar plants activate mechanisms to control sodium accumulation, which allows the maintenance of photosynthesis efficiency and the consequent growth of these plants under salt stress conditions. Our findings allowed us to analyze via an integrated manner the physiological, biochemical, anatomical, and molecular changes of rice cultivars, which are differentially susceptible to salinity. Thus, it will contribute to the rice breeding programs and the future production of this crop in stressful conditions.

2. Materials and methods

2.1. Plant material and growth conditions

The BRS Esmeralda (ES) and São Francisco (SF) rice cultivars were selected for this research because they showed more distinct salinity tolerance in pre-test under salt conditions (80 mM NaCl), with SF being more tolerant to salinity. Fig. S1 offers the principal component analysis (PCA) of seven growth and photosynthesis parameters from five rice cultivars (BRS Esmeralda, BRS Pepita, BRS Primavera, BRS Sertanejo, and São Francisco). It reveals the salinity tolerance contrast between SF and ES cultivars. The SF and ES seeds were supplied from Instituto Agronômico de Pernambuco (IPA).

The seeds were sown in vermiculite moistened with distilled water. Seven days old seedlings were placed in a hydroponic system containing a nutrient solution (Clark, 1975) oxygenated with aquarium pumps (dissolved oxygen of 7.5 ± 0.3 ppm). After seven days more, half of the plants were transferred to buckets (two plants per bucket) containing nutrient solution added NaCl (salt stress). Only the first salt-treatment application, the salt-treatment was divided into two daily doses to avoid osmotic shock and reaching the final concentration of 80 mM NaCl. This NaCl concentration was used because it generates salt stress capable of strongly inhibiting the growth of rice plants without them dying (Lopes et al., 2020). The other half of the plants remained in the nutrient solution without NaCl (control condition), and the pH solution was monitored daily and adjusted to 6.0 as needed. Besides, nutrient solutions were renewed every three days to avoid nutritional deficiency. During the experiment, the greenhouse conditions were as following: midday photosynthetic photon flux density (PPFD) approximately 1200 μmol m^{-2} s^{-1}, mean temperature of 32.2 ± 2 °C during the day and 25.9 ± 1 °C at night and mean relative humidity of 63.4 ± 16 %. The harvests were performed at 0, 12, 24, 48 h after exposure to NaCl only for real-time quantitative PCR (qPCR) analysis and at 6 and 12 days for physiological, biochemical, anatomical essays.

2.2. Experimental design and statistical analysis

The experimental design was completely randomized in factorial scheme 2 × 2, comprising two rice cultivars (ES and SF) and two growth conditions [control (0 mM NaCl) and salinity (80 mM NaCl)]. Each treatment was established with five repetitions of two plants, except for *gene* expression analysis conducted with only three repetitions with two plants. The data were submitted to a two-way analysis of variance (ANOVA), F-test ($p < 0.05$), and the mean values were compared by the Tukey test ($p < 0.05$). Statistical analyses were performed using the Sisvar® 5.3 software.

2.3. Growth parameters

The plants from each treatment were individually harvested. The leaf area was measured using a LI-3000 leaf area meter (LI-COR, Inc. Lincoln, NE, USA). Subsequently, plant material was separated into two groups. In the first group, one plant of each repetition was divided into leaves, roots, and stems for drying in a forced-air circulation oven at 60 °C for

48 h, then the dry mass was determined. In the second group, the fresh tissues of leaves and roots of the other plant of the same repetition were frozen immediately in liquid nitrogen and kept at -80 °C for biochemical analysis.

2.4. Gas exchange and chlorophyll a fluorescence

Gas exchange and chlorophyll *a* fluorescence measurements were performed in fully expanded leaves under constant CO_2 concentration and PPFD of 400 µmol mol^{-1} CO_2 and 1200 µmol photons m^{-2} s^{-1}, respectively. Before harvesting, gas exchanges [stomatal conductance (g_s), CO_2 assimilation (A), and transpiration (E)] were determined on the first fully expanded leaf from the apex using an infrared gas analyzer - IRGA (LI-6400XT, LI-COR, USA) coupled with artificial light. The carboxylation efficiency of ribulose-1,5-bisphosphate carboxylase/oxygenase (Rubisco) was estimated by the ratio *A/Ci*. Others parameters were also evaluated using a fluorometer (6400-40, LI-COR, USA) coupled to IRGA in dark-adapted leaves, as effective quantum yield of PSII [ΦPSII = (Fm′ − Fs)/Fm′], non-photochemical quenching [NPQ = (Fm − Fm′)/Fm′], photochemical quenching [qP = (Fm′ − Fs)/(Fm′ − Fo′)], maximum quantum yield of photosystem II (PSII) in dark-adapted leaves [Fv/Fm = (Fm − Fo)/Fm], energy excess at the PSII level [EXC = (Fv/Fm) - (ΦPSII)/(Fv/Fm)], and electron transport rate [ETR = (ΦPSII × PPFD × 0.5 × 0.84)] (Araújo et al., 2018).

2.5. Photosynthetic pigments

The chlorophyll *a* (Chl *a*), chlorophyll *b* (Chl *b*), and carotenoids were extracted in dimethyl sulfoxide (DMSO) saturated with $CaCO_3$ for 48 h at room temperature. Afterward, the samples were incubated at 65 °C in a water bath for 45 min (Barnes et al., 1992). Photosynthetic pigments were spectrophotometrically measured by absorbance reading at 480 nm, 649 nm and 665 nm, and the concentrations were calculated through the following equations: Chl $a = 12.47A_{665} - 3.62A_{649}$; Chl $b = 25.06A_{649} - 6.50A_{665}$; total chlorophyll (Chl *total*) $= 5.97A_{665} + 21.44A_{649}$, and carotenoids $= (1000A_{480} - 1.29$ Chl $a - 53.78$ Chl $b)/220$ (Wellburn, 1994).

2.6. Chloroplast ultrastructure

For ultrastructure observation, fresh leaves (last fully expanded leaf) were cut into 0.05 M sodium phosphate buffer (pH 7.2) containing 2.5 % glutaraldehyde (v/v) and 4 % paraformaldehyde. The fixed samples were washed in 0.05 M sodium phosphate buffer (pH 7.4) and post-fixed in 1 % (w/v) osmium tetroxide (OsO_4). After dehydration in a graded series of acetone solutions, the samples were embedded in epoxy resin (EMbed 812) according to Yamane et al. (2012) with some modifications. Ultrathin cuts were collected on 300-mesh copper grids, then stained with 2 % uranyl acetate and 0.5 % lead citrate. The chloroplast structure was observed using a transmission electron microscope (TEM, JEOL model JEM 101) at 100 kV.

2.7. Ions contents and Na^+ and K^+ loading in xylem sap

Extracts were obtained after homogenization of 50 mg of the dry mass (DM) of leaves and roots in 5 mL deionized water at 95 °C for 1 h and centrifuged at 3.000 x g for 10 min. The Na^+ and K^+ contents were determined by flame photometry (Micronal®, model B462), according to Malavolta et al. (1989). Xylem sap was collected from plants, according to Pandolfi et al. (2012). The roots were cut about 2 cm above the shoot-root junction and placed in a pressure chamber (Scholander-PMS Instrument Company, USA). A sufficient pressure (10–25 bar) for xylem sap exudation was applied. Then, the K^+ and Na^+ were measured in crude exudate by flame photometry, as described above.

2.8. Detection of Na^+ by confocal microscopy

Fully expanded leaves from the sixth nodes of both ES and SF rice cultivars subjected to control conditions and 80 mM NaCl were collected at days 6 and 12. Leaf-blade samples were taken halfway between the midrib and leaf margin and free-hand sectioned. Cross-sections at ~20 µm thick were made with a double-edged razor blade and petiole pith from *Cecropia* sp., which was used for holding the leaf blade sample (Silva et al., 2013).

For the characterization of the leaf blade's general anatomy under light microscopy, previously to the confocal microscopy analyses, some sections were stained with Astra blue and safranin as follows. Sections were cleared with 50 % household bleach, washed three times each 10 min with distilled water, stained with a mixture of 1 % Astra blue and 0.05 % safranin for 2 min, and mounted in distilled water (Johansen, 1940; McVeigh, 1935). Observations in unstained sections were also made. Photographs of the samples were then taken using a digital camera (UC 30; Olympus, Hamburg, Germany) attached to a light microscope (BX 41 T F; Olympus, Tokyo, Japan).

For the confocal microscopy analyses, sections were placed on 0.01 M phosphate-buffered saline (PBS) at pH 7.4 (Sigma-Aldrich) and later incubated with a cell membrane permeable cytosolic Na^+ indicator, 5 µM Asante NaTRIUM Green-2 AM, for 1 h in the dark (Lamy and Chatton, 2011; Roder and Hille, 2014). Fluorescence emission by Asante NaTRIUM Green-2 AM was collected from 535 to 555 nm. Sections were washed three times each 5 min with PBS and incubated with Calcofluor White (0.2 µg/mL) (Fluorescent Brightener 28, Sigma, UK) for 5 min in the dark. Fluorescence emission by calcofluor white is blue and indicates cellulose in the cell walls. Sections were then washed three times each 5 min with PBS, mounted in PBS at pH 7.4, and sealed with commercial nail polish. Samples were analyzed on a confocal scanning laser microscope (LSM710, Carl Zeiss, Jena) using appropriated lasers. Images were captured with Zen software (Zeiss).

2.9. Gene expression analysis

Total RNA was isolated from root tissues using an SV Total RNA isolation system (Promega, USA), according to the manufacturer's instructions. The concentration of total RNA was measured through a Nanodrop2000 spectrophotometer (Thermo Scientific, Waltham, USA), and its purity was checked by analyzing the A_{260}/A_{280} and A_{260}/A_{230} absorbance ratios. First-strand cDNA was synthesized employing the M-MLV Reverse Transcriptase (Promega), according to the manufacturer's protocol. The relative expression of marker genes related to Salt Overly Sensitive (SOS) and Na^+/H^+ exchanger (NHX) was made from the specific primer sets previously reported in the literature. The specific primer (*OsSOS1*-3 and *OsNHX1*-6) and reference *gene* (*OsUBQ*5) were synthesized as described by Çelik et al. (2019), Passricha et al. (2019), Fu et al. (2018), and Zhang et al. (2018) (Table S1). qPCR was performed on a Mastercycler ep realplex 4S (Eppendorf, Germany) using GoTaq®qPCR Master Mix. Relative expression was calculated employing the cycle threshold (CT) $2^{-\Delta\Delta C}{}_T$ method (Livak and Schmittgen, 2001).

3. Results

3.1. Negative impacts of salt stress on growth

Salt stress limited the growth of rice plants of both cultivars (Table 1). Salinity severely decreased the leaf area of both cultivars at six days of stress, and it was more pronounced at 12 days. Under saline and non-saline conditions, SF plants had a larger leaf area than ES, and the reductions caused by salinity in SF were also smaller than ES. The ES cultivar's leaf areas were reduced by salinity about 51 and 87 % at 6 and 12 days of stress, respectively. While in SF cultivar, these reductions were 44 and 64 %, respectively. Besides, salt stress reduced the dry masses of leaves, stems, and roots. The losses of the leaves dry mass in

Table 1
Leaf area and dry masses of leaves, stems, roots, and total dry mass of plants of BRS Esmeralda (ES) and São Francisco (SF) rice cultivars under absence (Control) and presence of 80 mM NaCl (Salt stress) for 6 and 12 days of treatments (DT).

DT	Cultivar	Leaf area (cm^2)		Dry mass (g $plant^{-1}$)							
				Leaves		Stems		Roots		Total	
		Control	Salt stress	Control	Salt stress	Control	Salt stress	Control	Salt stress	Control	Salt stress
6	ES	39.89 Ab	19.52 Bb	0.40 Ab	0.16 Bb	0.13 Ab	0.14 Ab	0.15 Ab	0.10 Bb	0.68 Ab	0.40 Bb
	SF	64.40 Aa	36.10 Ba	0.57 Aa	0.32 Ba	0.19 Aa	0.20 Aa	0.18 Aa	0.15 Ba	0.94 Aa	0.67 Ba
12	ES	173.18 Ab	23.21 Bb	1.12 Ab	0.20 Bb	0.34 Ab	0.18 Bb	0.35 Ab	0.18 Bb	1.81 Ab	0.56 Bb
	SF	270.25 Aa	98.70 Ba	1.81 Aa	0.68 Ba	0.64 Aa	0.37 Ba	0.51 Aa	0.38 Ba	2.96 Aa	1.43 Ba

The data represent the mean of five replicates. According to the F test ($p < 0.05$), all parameters show significant interaction between salinity and cultivars, except stems dry mass at 6 and 12 days. On the same analysis time, the upper-case letters compare the salinity treatments within each rice cultivar, and the lower-case letters compare the rice cultivar within each salinity treatment, according to the Tukey test ($p < 0.05$).

the ES cultivar were 60 and 82 %, while in the SF cultivar, these reductions were 44 and 62 %, at 6 and 12 days of stress, respectively (Table 1). There was no change in the stem dry mass of both cultivars at six days of stress, but at 12 days, salinity reduced it 47 and 42 % in the ES and SF cultivars, respectively. Also, the reductions in ES cultivar root dry mass due to salt stress were 33 and 49 %, while in the SF cultivar, these reductions were 17 and 25 %, at 6 and 12 days of stress, respectively. As a result of these changes caused by salinity, the ES cultivar's total dry mass was reduced by 41 and 69 % at 6 and 12 days, respectively. Nevertheless, in SF cultivar, such reductions were 29 and 52 % at 6 and 12 days, respectively. These results confirmed the better phenotypic appearance of SF plants observed under salt stress (Fig. 1), maintaining a better growth from roots to leaves than ES.

3.2. Differential changes in photosynthetic parameters by salinity

Salinity promoted considerable reductions in *A*, g_s, *E*, and *A/Ci* of both cultivars at all analyzed times (Fig. 2). Although this occurred, in general, the decreases caused by salt stress were less severe in SF plants. Reductions in *A*, g_s, *E*, and *A/Ci* in ES cultivar were 64, 74, 55, and 60 % at six days, respectively, and 52, 78, 59, and 37 % at 12 days (Fig. 2). In SF cultivar, these reductions were 47, 26, 16, and 60 % at six days, respectively, and 33, 38, 62, and 22 % at 12 days.

In general, salt excess in the root environment also harmed the φPSII, qP, and ETR (Fig. 3a, c, f). However, harm to these parameters was less evident or did not occur in SF plants. At six days, φPSII, qP, and ETR of ES cultivar were 27, 06, and 25 % lower under salinity, respectively. While in SF cultivar, reductions of 13 and 12 % occurred only in φPSII and ETR, respectively. At 12 days, the φPSII, qP, and ETR in the ES cultivar reduced 33, 17, and 39 % by salinity, respectively, while in the SF cultivar, only φPSII and ETR reduced 8 and 11 %, respectively. Additionally, it was possible to notice that salinity caused increases in the NPQ and EXC in both cultivars, being more evident in ES plants (Fig. 3b, e). In ES cultivar, these increases of NPQ and EXC were 62 and 24 % at six days, respectively, and 71 and 31 % at 12 days. On the other hand, the values of NPQ and EXC in SF plants under salinity were 12 and 8 % higher, respectively, than those under control at six days and 48 and 7 % higher at 12 days. Otherwise, salinity provoked no significant changes in the Fv/Fm (Fig. 3d).

There was not chlorophyll degradation caused by salinity in both cultivars (Table 2). The cultivar ES showed an increase of 16, 20, and 15 % in Chl *a*, Chl *b*, and Chl *total* contents, respectively, under salinity at six days. Meanwhile, salinity induced a 22 % increase in Chl b at 12 days in the SF cultivar. On the other hand, salinity caused the degradation of 52 and 7 % of carotenoids in ES cultivar at 6 and 12 days, respectively. Furthermore, an 18 % reduction in carotenoids in the SF cultivar occurred only at six days.

The TEM images displayed changes in the chloroplast ultrastructure of ES and SF cultivars under salinity (Fig. 4). In general, the salinity caused disorganization in the lamellar system (Fig. 4b, d, f, and h), and grana and lamellae showed slightly swollen concerning controls. There was also damage in thylakoid stacking (Fig. 4d, h). Starch grains and plastoglobuli accumulation was observed in plants under salt stress. These changes in chloroplast ultrastructure induced by salinity were more remarkable in ES (Fig. 4b, d) than in SF plants (Fig. 4f, h). Also, it was possible to observe the dissolution of grana and the envelope's

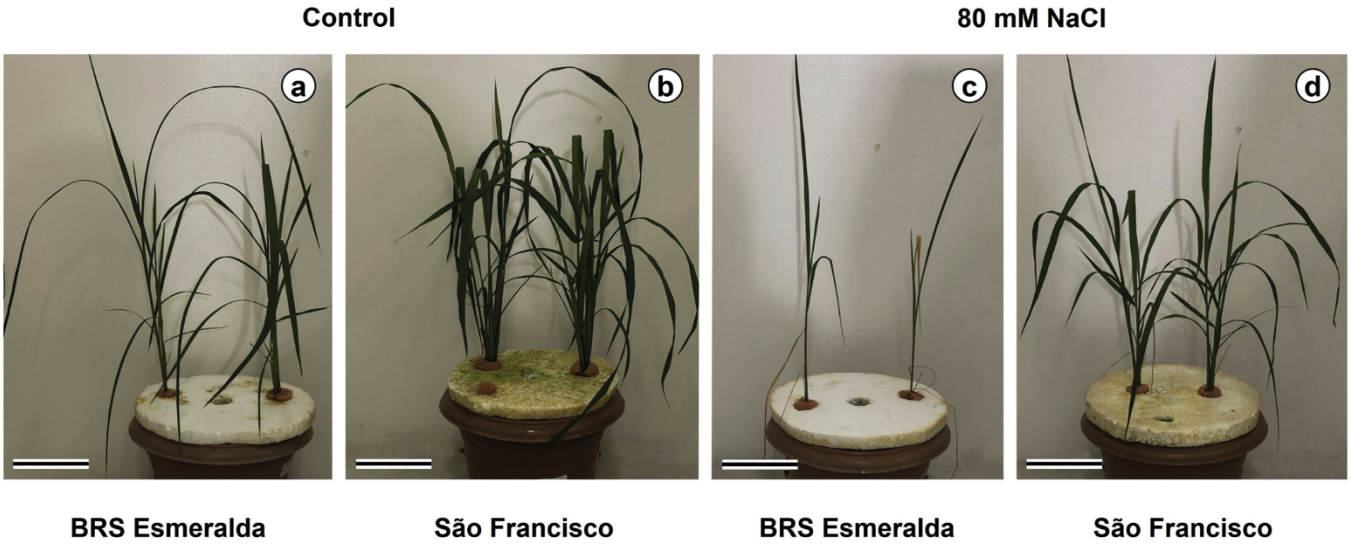

Fig. 1. Phenotypes of BRS Esmeralda and São Francisco rice cultivars cultivated under absence (control; **a**, **b**) and presence of 80 mM NaCl (**c**, **d**) for 12 days. *Scale bars*, 10 cm.

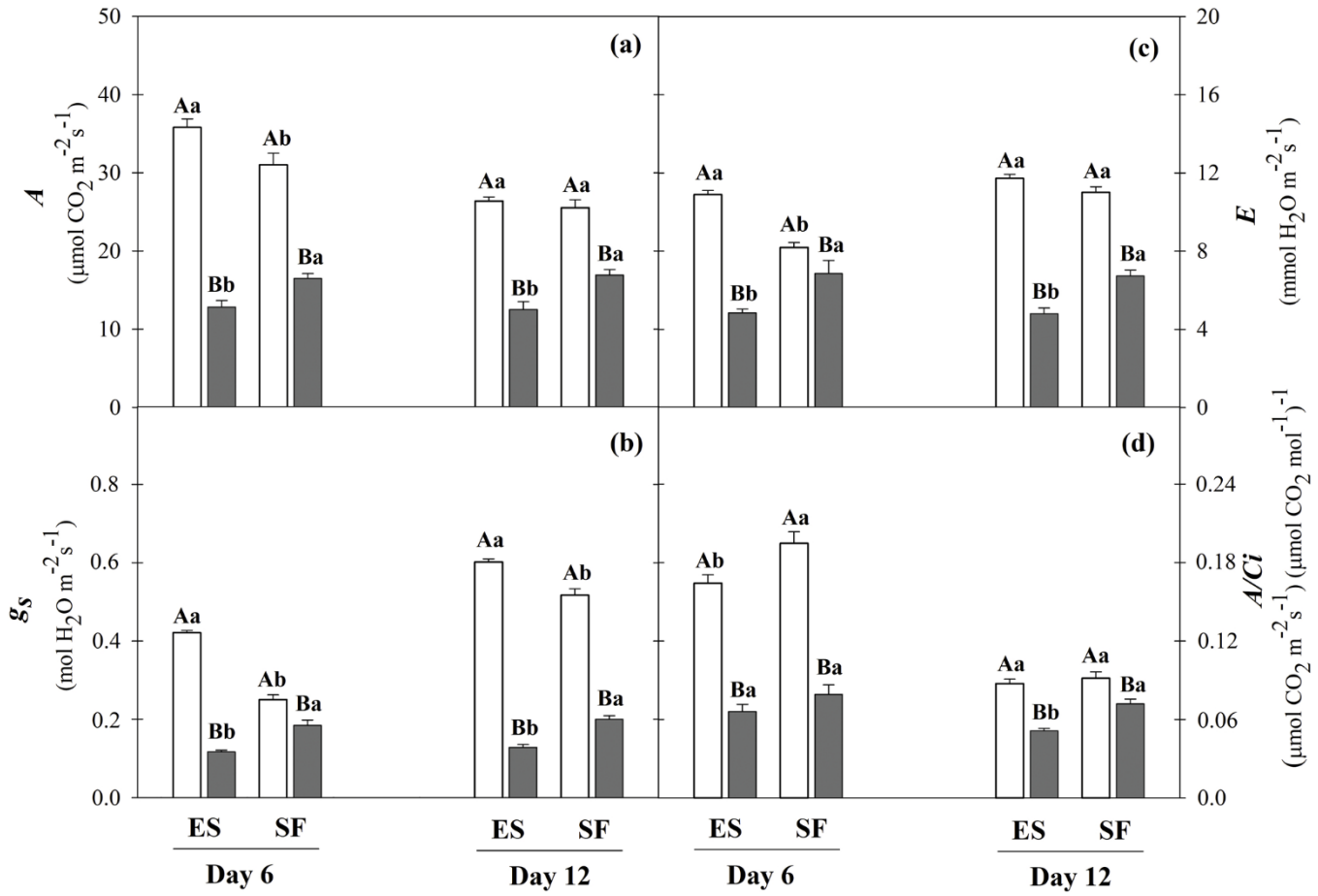

Fig. 2. CO_2 assimilation rate (*A*, **a**), stomatal conductance (g_s, **b**), transpiration rate (*E*, **c**), and carboxylation efficiency of Rubisco (*A/Ci*, **d**) of BRS Esmeralda (ES) and São Francisco (SF) rice cultivars grown under absence (*white bar*) and presence (*gray bar*) of 80 mM NaCl for 6 and 12 days. The data represent the mean of five replicates. According to the F test ($p < 0.05$), all parameters show significant interaction between salinity and cultivars. On the same analysis time, the upper-case letters compare the salinity treatments within each rice cultivar, and the lower-case letters compare the rice cultivar within each salinity treatment, according to the Tukey test ($p < 0.05$).

disruption in ES plants, mainly at 12 days (Fig. 4d).

3.3. Ionic homeostasis

Salinity significantly reduced the K^+ contents in leaves and roots of both cultivars at 6 and 12 days of salt stress (Fig. 5a, b). In general, the reductions caused by salt stress were less severe in SF plants. In ES cultivar, the reductions in K^+ contents in leaves and roots were 40 and 13 % at six days, respectively, and 51 and 59 % at 12 days. While in SF cultivar, the reductions in K^+ contents in leaves and roots were 14 and 31 % at six days, respectively, and 24 and 42 % at 12 days. The salinity decreased 54 and 22 % of K^+ contents in the xylem sap at six days of ES and SF cultivars, respectively (Fig. 5c). Nevertheless, at 12 days, the K^+ content was reduced by 26 % only in ES.

The plants accumulated more Na^+ in the tissues and xylem sap due to salt stress (Fig. 5d–f). Nevertheless, in general, the SF plants showed smaller increases in Na^+ content than ES plants. In ES leaves, these increases were 511 and 536 % at 6 and 12 days, respectively, while in SF leaves, they were 117 and 281 % (Fig. 5d). In ES roots, the salt stress increased Na^+ content by 276 and 574 % at 6 and 12 days, respectively, while in SF roots, they were 256 and 559 % (Fig. 5e). The salinity increased Na^+ content in xylem sap of ES by 129 and 55 % at 6 and 12 days, respectively. In comparison, Na^+ content in xylem sap of SF was only 85 and 15 % higher at 6 and 12 days, respectively, under salt stress (Fig. 5f).

The general anatomy of the leaf blade of the rice plants, as observed in unstained (Fig. 6a) and stained (Fig. 6b) sections, revealed a single-layered epidermis presence bulliform cells on the adaxial surface and homogenous mesophyll. The vascular bundles were composed of xylem (metaxylem and protoxylem) and phloem, surrounded by a bundle sheath. Sclerenchyma bundles right below the epidermis were observed on the adaxial and abaxial sides of the vascular bundles. Some sections showed intact protoxylem (Fig. 6b) while others, protoxylem lacunae (Fig. 6a). As both rice cultivars take similar leaf anatomy, only the ES cultivar was shown.

The Na^+ accumulation pattern in leaves was inspected by confocal microscopy utilizing a Na^+ fluorescent probe (Fig. 6c–j). Green fluorescence was observed in the controls (Fig. 6c, e, g, and i) as well as salt-stressed plants (Fig. 6d, f, h, and j) at days 6 and 12. The Na^+ presented on the outer periclinal walls of epidermal cells, on the adaxial surface, except for the bulliform cells. On the abaxial side, in the cell walls of both metaxylem and sclerenchyma cells, and within the chlorenchyma cells (Fig. 6c–j). It is essential to mention that the protoxylem, phloem cells, and vascular bundle sheath cells did not show any green fluorescence. Plants from both cultivars under salt-stressed (Fig. 6d, f, h, and j) showed a more apparent green fluorescence than controls (Fig. 6c, e, g, and i) at both times of collection. However, Na^+ was even more intense in ES plants under saline stress (Fig. 6f) than in the controls (Fig. 6e) at day 12. Na^+ accumulation seems to move from the metaxylem to the chlorenchyma cells. When comparing plants under salt stress at day 6 (Fig. 6d, h) and day 12 (Fig. 6f, j) of both cultivars, the green intensity becomes less bright in the metaxylem and brighter the chlorenchyma

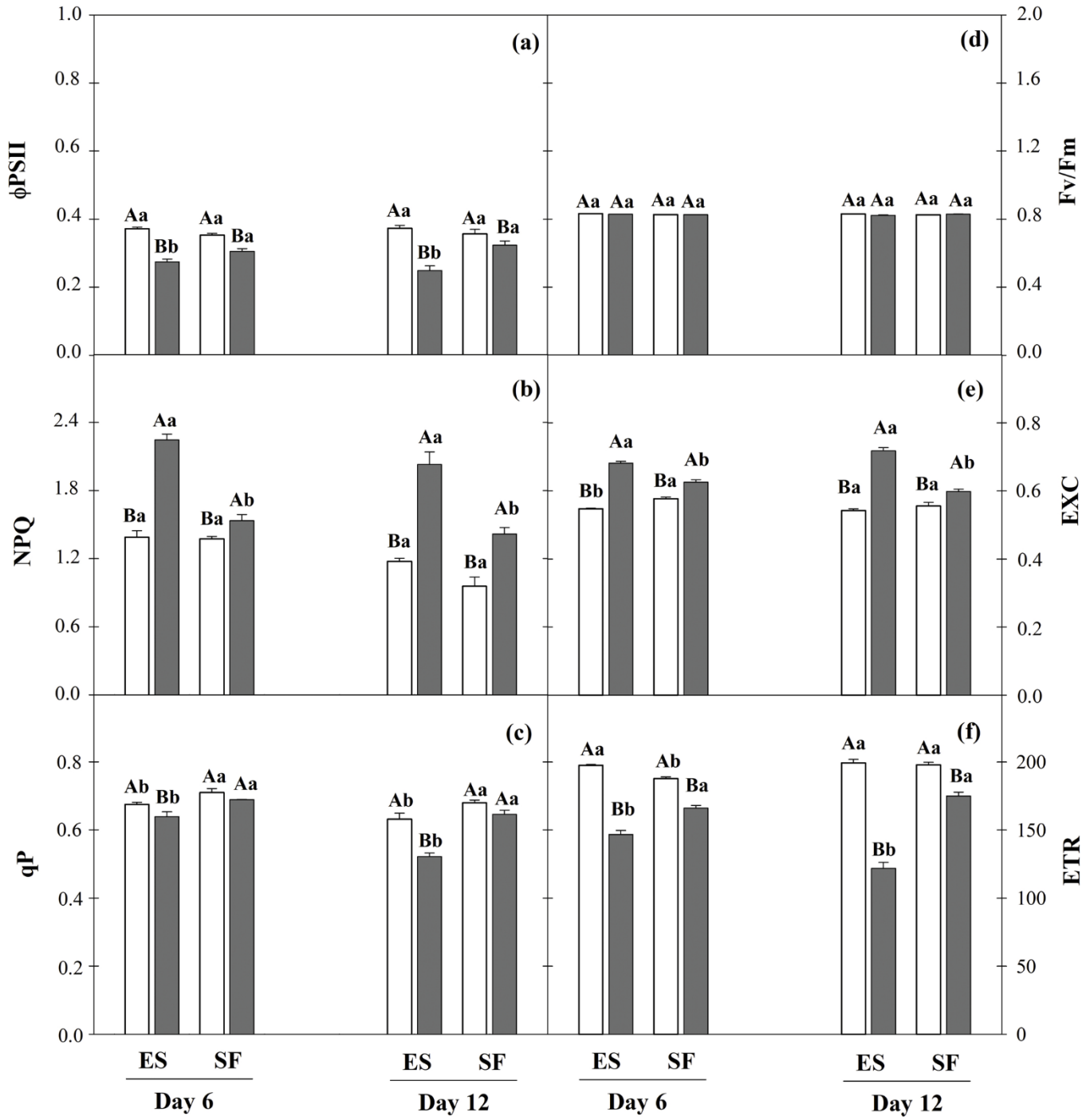

Fig. 3. Effective quantum yield of PSII (ϕPSII, **a**), non-photochemical quenching (NPQ, **b**), photochemical quenching (qP, **c**), photosystem II maximum efficiency (Fv/Fm, **d**), energy excess at the PSII level (EXC, e), and electron transport rate (ETR, **f**) of BRS Esmeralda (ES) and São Francisco (SF) rice cultivars grown under absence (*white bar*) and presence (*gray bar)* of 80 mM NaCl for 6 and 12 days. The data represent the mean of five replicates. According to the F test ($p < 0.05$), all parameters show significant interaction between salinity and cultivars, except Fv/Fm (d). On the same analysis time, the upper-case letters compare the salinity treatments within each rice cultivar, and the lower-case letters compare the rice cultivar within each salinity treatment, according to Tukey test ($p < 0.05$).

cells.

3.4. Gene expression of ion transporters

To investigate the differential Na^+ accumulation in the ES and SF cultivars under salinity, the transcription level of nine genes *(OsSOS1, OsSOS2, OsSOS3, OsNHX1, OsNHX2, OsNHX3, OsNHX4, OsNHX5*, and Os*NHX6*) related to the regulation, transport, and, consequently, Na^+ ionic homeostasis was evaluated (Fig. 7). In general, salinity induced the activation of the SOS pathway in rice roots. At 12, 24, and 48 h of the onset of salt stress, the *OsSOS1* and *OsSOS2* genes' relative expression was markedly higher under salt stress, mainly in SF cultivar (Fig. 7a, b). On average, the abundance of the *OsSOS1 gene* in SF plants was 2.7 times higher than ES cultivar under saline environment, while that of the *OsSOS2 gene* was 1.6 times higher. Differently, the relative expression of the *OsSOS3 gene* was lower or remained unchanged by salinity, except after 24 h of salt stress in SF plants, in which the *gene* abundance was 2.0 times higher than the control condition (Fig. 7c). However, the levels of

Table 2
Chlorophyll (Chl) *a*, *b* and *total*, and carotenoids content in plants of BRS Esmeralda (ES) and São Francisco (SF) rice cultivars under absence (Control) and presence of 80 mM NaCl (Salt stress) for 6 and 12 days of treatments (DT).

DT	Cultivar	Contents (mg g^{-1} DM)							
		Chl *a*		Chl *b*		Chl *total*		Carotenoids	
		Control	Salt stress	Control	Salt stress	Control	Salt stress	Control	Salt stress
6	ES	14.30 Ba	16.53 Aa	4.62 Ba	5.55 Aa	19.32 Ba	22.19 Aa	12.99 Aa	6.18 Bb
	SF	10.86 Ab	11.55 Ab	3.38 Ab	3.41 Ab	14.38 Ab	15.09 Ab	12.35 Aa	10.08 Ba
12	ES	13.46 Ab	12.99 Ab	4.65 Ab	4.80 Ab	18.28 Aa	17.83 Ab	65.18 Aa	60.53 Bb
	SF	14.35 Aa	14.27 Aa	5.29 Ba	6.43 Aa	19.69 Aa	20.82 Aa	66.21 Aa	66.56 Aa

The data represent the mean of five replicates. According to the F test ($p < 0.05$), all parameters show significant interaction between salinity and cultivars. On the same analysis time, the upper-case letters compare the salinity treatments within each rice cultivar, and the lower-case letters compare the rice cultivar within each salinity treatment, according to the Tukey test ($p < 0.05$).

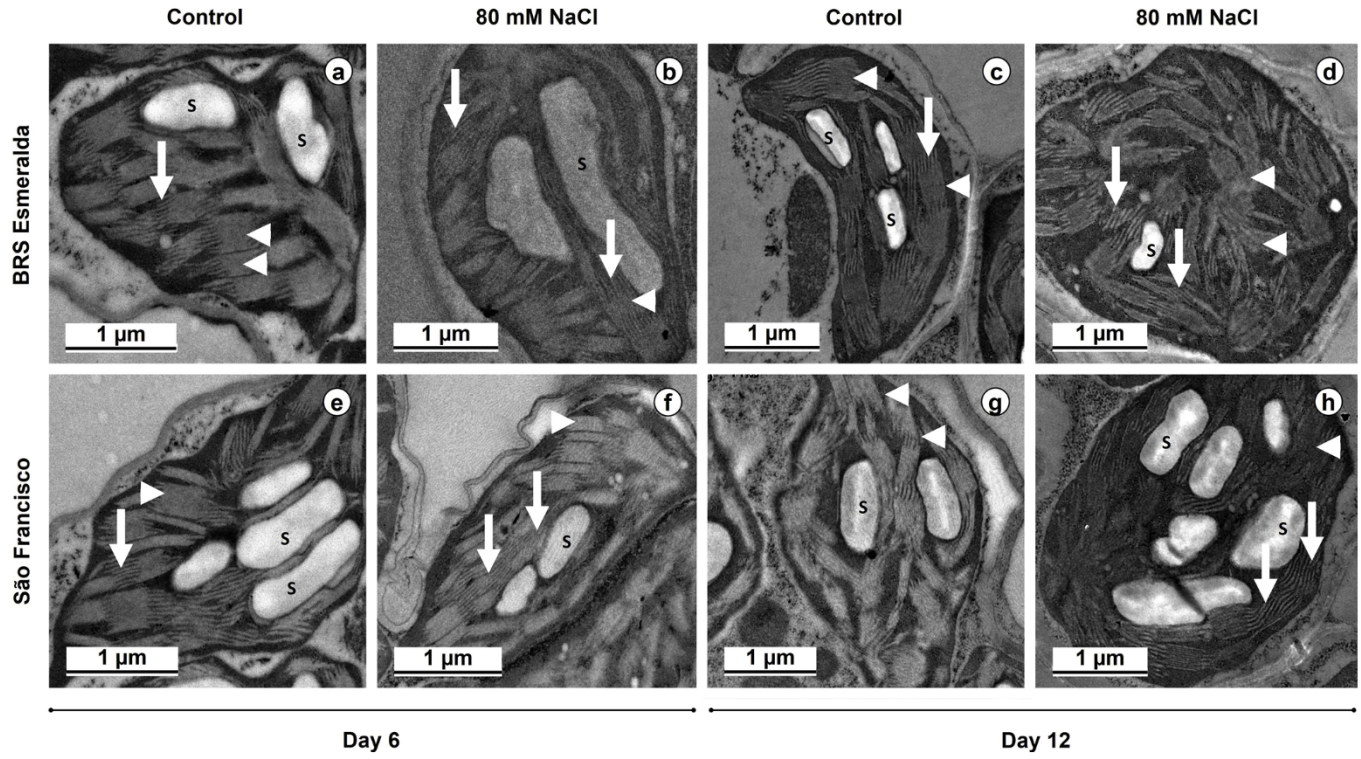

Fig. 4. Chloroplast ultrastructure of BRS Esmeralda and São Francisco rice cultivars grown under absence (control) and presence of 80 mM NaCl for 6 and 12 days. Note the disorganization in the lamellar system of BRS Esmeralda rice cultivar plants grown under salt stress (**b**, **d**) compared to the ones in the control plants (**a**, **c**). The disorganization is most noticeable at day 12 (**d**), when thylakoid stacking clearly shows damage and plastoglobuli accumulation. The same pattern of structural changes in the lamellar system caused by the salinity is observed for the São Francisco rice cultivar grown under salt stress (**f**, **h**) compared to the ones control plants (**e**, **g**). S, starch grain; arrow, grana; arrowhead, stroma thylakoid (stroma lamellae).

OsSOS3 transcription under salinity at all times evaluated were higher in SF plants than ES plants.

The *OsNHX4* and *OsNHX6* genes were not responsive to salinity in the two rice cultivars, but the *OsNHX1*, *OsNHX2*, *OsNHX3*, and *OsNHX5 gene* expressions were all induced (Fig. 7d–g). The *OsNHX1* expression was higher under salinity in ES roots only at 48 h of salinity exposure, 1.12 times higher. In comparison, it was higher in SF since 12 h, and the *OsNHX1* expression was higher in SF than ES under salinity at all times of analysis, being 91 % higher on average (Fig. 7d). The *OsNHX2* genes were not overexpressed in ES cultivar under salt stress. In contrast, *OsNHX2* in SF cultivar was overexpressed at 24 and 48 h after saline treatment (Fig. 7e). Its relative expression after 24 h was, on average, 18.4 times higher than ES plants under salinity and 4.0 times higher than SF in the absence of salinity. The salinity reduced *OsNHX3* expression only in 12 h, but it significantly enhanced *OsNHX3* expression at 24 and 48 h (Fig. 7f). Also, at 24 and 48 h of stress enforcement, the mRNA abundance of *OsNHX3* was 17 and 39 % higher in SF cultivar than in ES cultivar under salt stress and, on average, *OsNHX3* expression was 1.2 and 1.3 times higher in SF and ES under salinity than non-saline condition, respectively (Fig. 7f). The salinity increased *OsNHX5* expression in ES cultivar until 24 h, an average increase of 91 % compared to control (Fig. 7g). In the SF cultivar, there was a considerable reduction in expression at 12 h caused by salt stress followed by overexpression at 24 h. In 48 h, *OsNHX5* expression was reduced by salinity in both cultivars. Besides, the cultivars showed a similar level of *OsNHX5* expression under salinity after 24 h.

4. Discussion

Plants growing under salt stress conditions face severe metabolism changes that impair their development. These disturbances culminate in considerable losses in productivity and generate environmental and economic impacts, especially in major crops such as rice (Hoang et al., 2016; Majeed and Muhammad, 2019). Nevertheless, some plant species

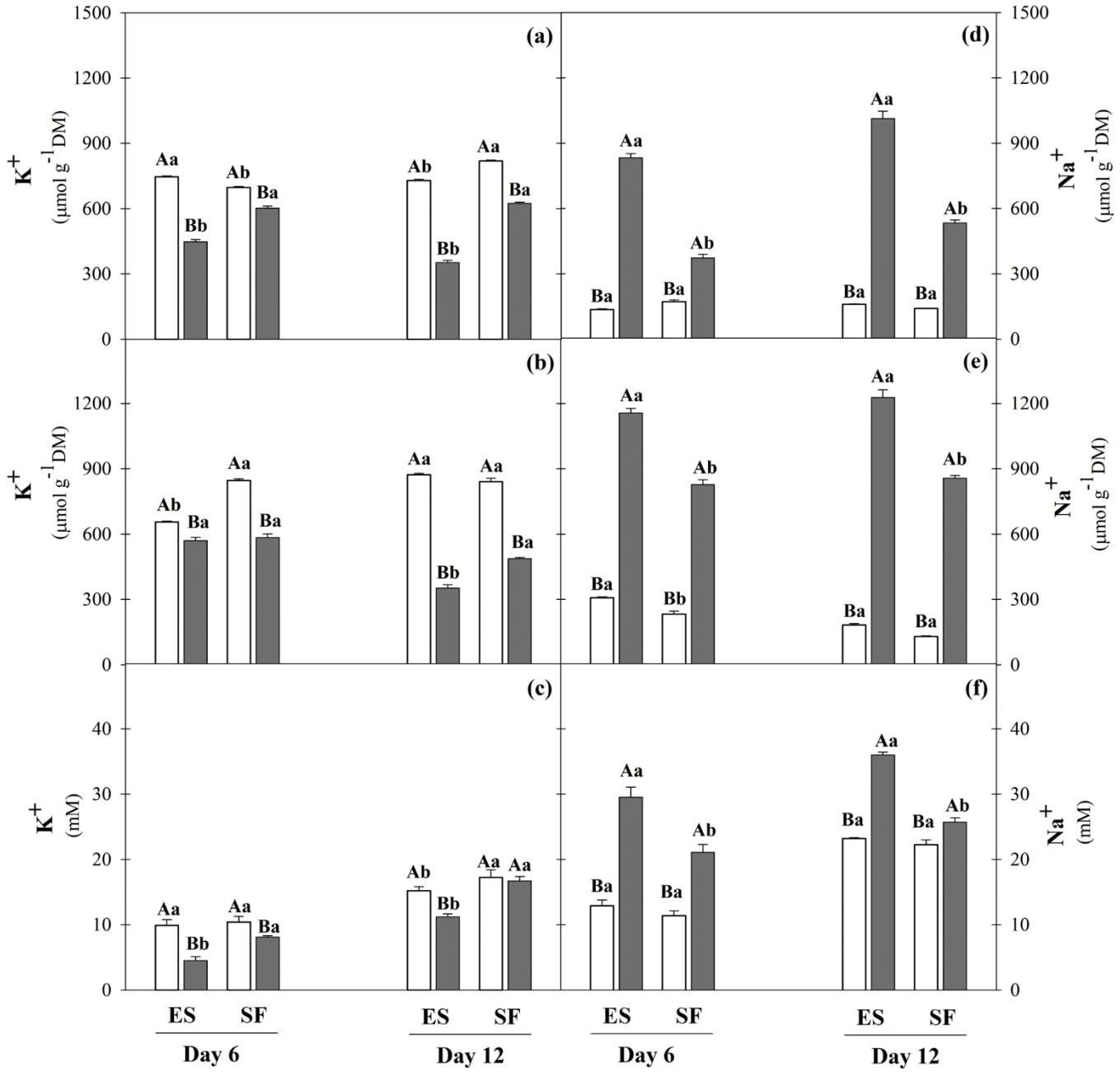

Fig. 5. K^+ and Na^+ content in leaves (**a, d**), roots (**b, e**), and xylem sap (**c, f**) of BRS Esmeralda (ES) and São Francisco (SF) rice cultivars grown under absence (*white bar*) and presence (*gray bar*) of 80 mM NaCl for 6 and 12 days. The data represent the mean of five replicates. According to the F test ($p < 0.05$), all parameters show significant interaction between salinity and cultivars. On the same analysis time, the upper-case letters compare the salinity treatments within each rice cultivar, and the lower-case letters compare the rice cultivar within each salinity treatment, according to the Tukey test ($p < 0.05$).

have developed a few tolerance mechanisms for minimizing or avoid damage imposed by salinity (Gupta et al., 2018; Riaz et al., 2019; Shahzad et al., 2019). Thus, this study evaluated the differential tolerance of two rice cultivars to salt stress and provided evidence about some physiological, biochemical, and molecular mechanisms effective for this phenomenon.

Salinity limited rice plants' growth (Table 1; Fig. 1). Furthermore, the most severe reductions imposed by salt stress in the leaf area, dry mass, and phenotypic appearance were more evident in the ES plants than in SF, indicating a differential sensibility to salinity. Many studies had already shown that this complex environmental adversity inhibits rice plants' growth (Chang et al., 2019; Fu et al., 2018; Gerona et al., 2019; Mirdar Mansuri et al., 2019; Tsai et al., 2019). These studies showed that different genotypes or varieties have contrasting salt stress tolerance by strictly regulated mechanisms. Maintaining productivity is due to adjustments in the main plant physiological processes, such as photosynthesis, protein synthesis, *gene* expression, ionic homeostasis, redox status, and metabolite levels. So, the type of acclimatization response to salt stress depends on the species, cultivar, and experimental conditions (Prisco et al., 2016).

4.1. Ultrastructure preservation is crucial for salt tolerance

For many plants, the principal physiological process affected by Na^+ toxicity is photosynthesis. Wherein all participating components of the photosynthetic machinery are potentially affected by salt stress, such as photosynthetic pigments, photosystems, electron transport systems, gas exchange processes, and enzymes involved in carbon metabolism.

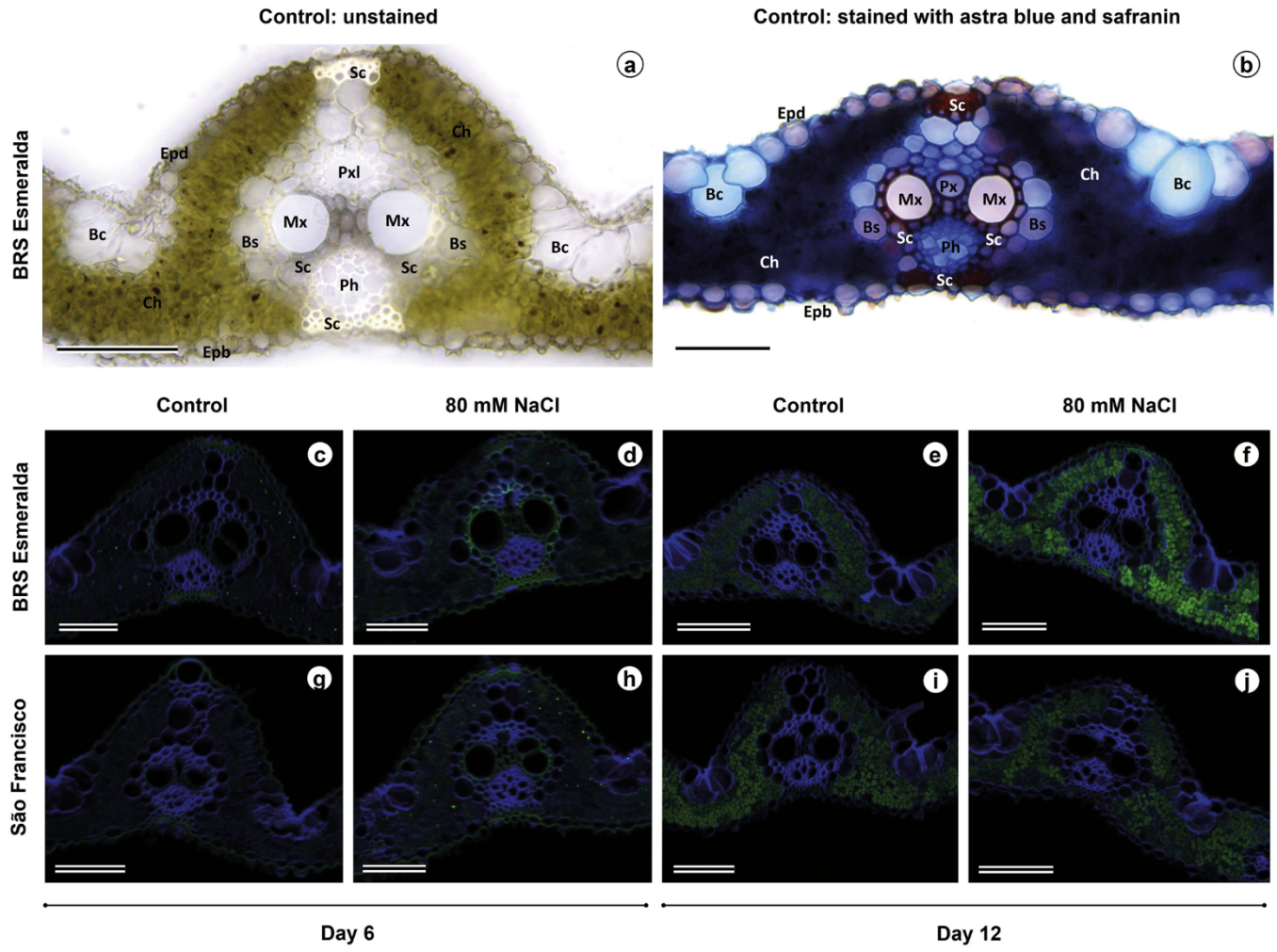

Fig. 6. Cross-sections of the leaf blade taken halfway between the midrib and leaf margin of BRS Esmeralda and São Francisco rice cultivars grown under absence (control) and presence of 80 mM NaCl for 6 and 12 days. General anatomy of BRS Esmeralda cultivar's leaf blade as observed under light microscope in an unstained section (**a**) and section stained with Astra blue and safranin (**b**). Subcellular localization of sodium (Na^+), with Asante NaTRIUM Green-2 AM and calcofluor-white (counterstain), in both rice cultivars grown under absence (control) and presence of 80 mM NaCl for 6 and 12 days as observed under confocal microscopy (**c** – **j**). Green and blue fluorescence indicate the presence of Na^+ and cellulose, respectively. Bc, bulliform cell; Bs, bundle sheath cell; Ch, chlorenchyma; Epb, epidermis on the abaxial side; Epd, epidermis adaxial side; Mx, metaxylem; Ph, phloem; Px, protoxylem; Pxl, protoxylem lacunae; Sc, sclerenchyma. *Scale bars* (**a**–j), 50 μm (For interpretation of the references to colour in this figure legend, the reader is referred to the web version of this article).

Therefore, any mechanism that relieves Na^+ toxicity in leaves and increases photosynthetic efficiency became essential for plant tolerance to salt stress (Ashraf and Harris, 2013; Nowicka et al., 2018). In this study, salinity drastically reduced gas exchange, impairing *A*, g_s, *E*, and *A/Ci* of rice plants, especially in the ES cultivar (Fig. 2). In SF plants, the damage caused by salinity on the gas exchange was less severe. It follows the results obtained by Radanielson et al. (2018), pointing out that the tolerant genotype required higher salinity levels than the sensitive genotype to reduce the net rates of photosynthesis and leaf transpiration by 50 %. Thus, our data suggest that in the SF cultivar, the process of fixing CO_2 was more effective, and more carbon was available to be invested in plant growth, which supported the better growth and development of this cultivar under salt stress conditions (Pan et al., 2016; Tang et al., 2018; Zhu et al., 2019).

There was no difference in Fv/Fm of plants under saline and non-saline conditions of both cultivars (Fig. 3d), indicating no photoinhibition (Mancarella et al., 2016). Salt stress, however, reduced the ΦPSII and ETR in both cultivars (Fig. 3). Such reductions were more pronounced in ES cultivar than SF, which evidence qP loss and an excess of reducing power associated with lower energy capture efficiency in open PSII reaction, leading to inhibition of electron transport and a notable thermal dissipation, observed by increased NPQ (Du et al., 2019; Miranda et al., 2016; Nie et al., 2018). Thus, SF plants presented lesser damage than ES plants, suggesting a better photosynthetic adaptation to preserve better the ΦPSII and ETR under salt stress (Fig. 3a, f), which led to a lower NPQ and EXC (Fig. 3b, e). Some previous studies had already reported a similar behavior when comparing other sensitive and tolerant salt-stress genotypes (Chutimanukul et al., 2018; Wang et al., 2019). In these studies, tolerance to salinity is associated with a better ability to prevent damage caused by excess energy and the maintenance of biochemical homeostasis in photosynthetic reactions, generating fewer biomass losses (Tsai et al., 2019).

Among the typical salt-stress damage, there is reducing of chlorophyll synthesis or pigment degradation, which compromises photosynthetic activity and, consequently, plant growth and development (Nie et al., 2018; Qu et al., 2012). However, at six days of the saline treatment, there was a chlorophyll increase in ES plants (Table 2), indicating an initial attempt to dispel excess excitation energy of the photosystems. Still, increasing the time of exposure to stress, this improvement was repealed without any effectual increment in qP. Indeed, SF plants still show lower chlorophyll than ES under salt conditions until six days but already maintained similar qP to control plants, which means a more

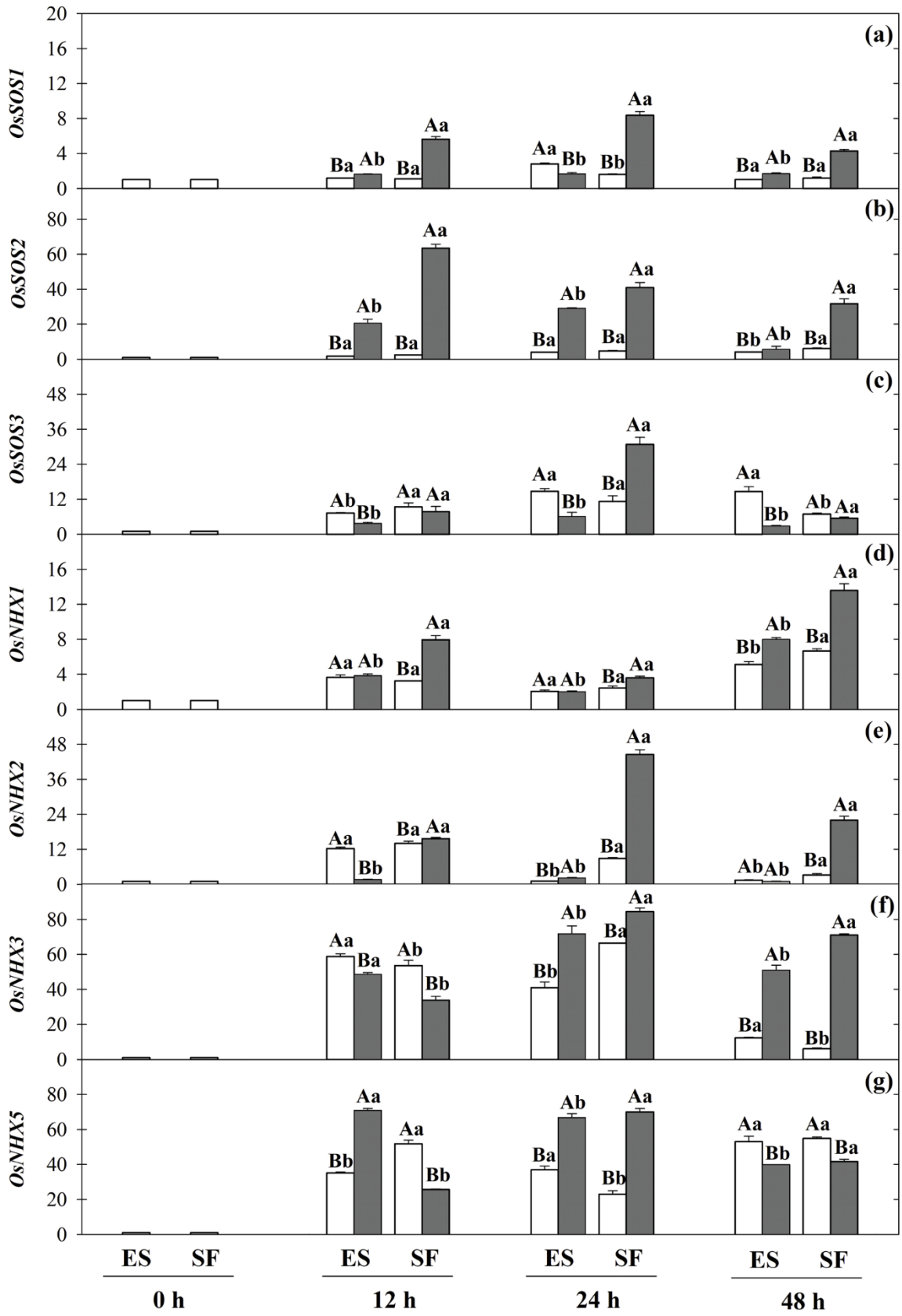

Fig. 7. Relative expression of the genes *OsSOS1* (**a**), *OsSOS2* (**b**), *OsSOS3* (**c**) *OsNHX1* (**d**), *OsNHX2* (**e**), *OsNHX3* (**f**), and *OsNHX5* (**g**) in roots of BRS Esmeralda (ES) and São Francisco (SF) rice cultivars grown under absence (*white bar*) and presence (*gray bar*) of 80 mM NaCl for 0, 12, 24 and 48 h. The data represent the mean of three replicates. According to the F test ($p < 0.05$), all parameters show significant interaction between salinity and cultivars, except *OsNHX3* at 12 and 24 h (f). On the same analysis time, the upper-case letters compare the salinity treatments within each rice cultivar, and the lower-case letters compare the rice cultivar within each salinity treatment, according to the Tukey test ($p < 0.05$).

efficient photoprotection mechanism against long-term salinity. The tolerance to salt stress of *Thellungiella salsuginea*, a halophyte plant, is also related to the more efficient use of excitation energy (Goussi et al., 2018). On the other hand, carotenoids can act as accessory pigments, as well as they can prevent photooxidative damage to chlorophyll molecules. Hence, the reduction of damage caused by salinity in SF, conserved the carotenoid contents, provides a photoprotective action to the photochemical apparatus and qP maintenance that supports better performance in front of salt stress (Table 2; Fig. 3c).

Damage to leaf anatomy and chloroplasts integrity eventually impair or even prevent the photosynthetic process under salt stress conditions (Du et al., 2019). Salt-tolerant plants, such as halophytes, maintain the structural integrity and arrangement of chloroplasts, which is essential for converting luminous energy into chemical energy (Bejaoui et al., 2016). Some of the damages induced in the chloroplast by salinity include the morphological deformations, like thylakoid swelling and envelope rupture, altering the appearance of some starch grains and some vesicles, probably originating from the dismantling of thylakoid, besides chloroplasts with a reduced number of the thylakoid (Araújo et al., 2021; Goussi et al., 2018). These salt-induced changes in chloroplast structure are linked to chlorophyll content changes, PSII efficiency, and chlorophyll fluorescence (Islam et al., 2019). In our study, ES plants grown in a saline environment presented losses in several of these traits, while SF plants showed less noticeable alterations, indicating minor damage to chloroplasts (Fig. 4). This finding suggests that the higher tolerance to salt stress observed in cultivar SF than ES is related to the better prevention of chloroplast ultrastructure.

4.2. Na^+ and K^+ uptake control is critical under salt stress

To understand the mechanisms that contribute to the differential tolerance between ES and SF cultivars, these rice cultivars' performance concerning ionic adjustment was assessed, which relates to the contrasting responses for tolerance or susceptibility to salt stress. Salt tolerant plants employ strategies to restrict the movement of cytotoxic Na^+ in growing and metabolically active plant organs, and they regulate the necessary ionic flow to maintain a high content of essential ions such as K^+ (Assaha et al., 2017; Chakraborty et al., 2019). Accordingly, in this study, SF plants under salt stress accumulated a lower Na^+ content in leaves and roots, generally it maintained higher K^+ content than the ES under the same conditions (Fig. 5a, b, d, e). Besides, leaves accumulated fewer Na^+ than roots, indicating a mechanism for regulating this toxic ion's translocation from the root system to the leaves, which was more efficient in SF. It may be supported by changes in Na^+ and K^+ concentration in the xylem sap of cultivars. Indeed, the SF suffered an initial reduction (at six days) in the K^+ concentration in xylem sap under salinity, but this does not occur at 12 days, indicating a rebalance in the K^+ concentration so that the SF cultivar has a K^+ concentration like the non-saline condition (Fig. 5c). The K^+ content reduction was lesser in the SF leaves than in the ES cultivar (Fig. 5a), which did not present K^+ concentration preservation in the xylem sap under salt stress conditions at 12 days (Fig. 5c). Under these same conditions, the SF cultivar also displayed less Na^+ concentration in the xylem sap than the ES cultivar; thus, Na^+ uptake was limited. Other researchers had already found equivalent results working with rice varieties (Gerona et al., 2019; Liu et al., 2019; Zhang et al., 2018). For example, Na^+ transport from the root to the aerial part was reduced in the Reiziq cultivar, considered salt-stress tolerant, due to a reduction in the capacity of Na^+ efflux in the root elongation zone through partial activation of the *OsSOS1 gene* (Liu et al., 2019) Additionally, low levels of Na^+ may benefit an increase of Ca^{2+} which contributes to salt stress tolerance (Zhang et al., 2018). Although calcium metabolism was not the focus of our study, it is another path to be explored in the future. Therefore, these findings support that SF cultivar tolerance may be related to mechanisms of exclusion or restriction to Na^+ influx at the root besides vacuolar compartmentalization (Zhang et al., 2018), and better maintenance of the K^+/Na^+ ratio compared to ES, evident in saline conditions in leaves, roots, and xylem sap (Fig. S2). This better control of the Na^+ and K^+ balance in SF is most evident by the K^+/Na^+ ratio higher than one in the leaves at both 6 and 12 days. Thus, the K^+/Na^+ ratio that is an indicator in selecting new winter wheat species with higher salt tolerance (Cheng et al., 2015) may also be a good indicator for rice genotypes.

The confocal microscopy fluorescence technique used to examine Na^+ dynamics in leaf tissues (Fig. 6) confirmed the leaf Na^+ content results (Fig. 5d). In response to salt stress, there was a more notorious Na^+ fluorescence signal in the leaves, especially in ES plants, which reinforces this cytotoxic ion's most considerable accumulation in this cultivar (Fig. 5d). Also, its relationship with salinity sensitivity. Analysis by confocal microscopy showed that Na^+ accumulation by the SF cultivar seems lower than the ES cultivar when the green intensity of both cultivars under salt stress is compared (Fig. 6f, j). Although it was stored mainly in the vacuole, Na^+ accumulation was specific to certain leaf sites, and not all cells accumulated Na^+ within the vacuole. That is quite noticeable as the parenchyma cells around the metaxylem, protoxylem, phloem, sheath bundle, and bulliform cells do not show Na^+ accumulation. As the metaxylem cells become active in grasses, protoxylem cells usually break or tear, giving rise to the protoxylem lacunae (Evert, 2006; Tucker, 1957). As we analyzed fully expanded leaves from the sixth nodes and the lifespan of protoxylem is short and restricted to young leaves, it is possible that the Na^+ was not located within such cells and neither in their walls because the cells had already been torn nor were not actives in water transport. However, high-intensity fluorescence points in the leaf sections are reported as a helpful marker of Na^+ in *Pongamia pinnata* under salt stress (Marriboina et al., 2017). Besides, it has been reported that cytosol Na^+ fluorescence intensity is higher in salt-sensitive wheat than in tolerant cultivars. However, the opposite occurs in the vacuole (Cuin et al., 2011).

Also, as the bulliform cells are the largest living cells observed in the section, and therefore with the largest vacuoles, one may expect that such cells would accumulate Na^+ (Fig. 6a, b). However, they do not constitute sites of Na^+ accumulation (Fig. 6f, j). Bulliform cells can rapidly take up or lose water (i.e., expanding and contracting); also, by forming longitudinal strips on the adaxial leaf surface, they have been implicated in the leaf rolling response in drought-stressed grasses (Kellogg, 2015; Matschi et al., 2020). Na^+ accumulation within bulliform cells could disturb the water balance necessary to control leaf rolling. Therefore, excluding Na^+ from bulliform cells may be a way to guarantee that plants growing under salt stress will still be able to roll their leaves and avoid other disturbances such as loss of water and heating of leaf tissues.

Several studies reported that the activation of the expression *SOS* and *NHX* genes is strongly associated with salt stress tolerance in different species, such as sorghum (Kandula et al., 2019; Miranda et al., 2017), maize (Huang et al., 2018), barley (Fu et al., 2018), tomato (Baghour et al., 2019), and in the rice itself (Bertazzini et al., 2018). In our study, in general, the expression of *OsSOS1*, *OsSOS2*, and *OsSOS3* genes increased in both cultivars from the onset of salt stress (Fig. 7a–c). Nevertheless, in rice plants of the SF cultivar, the abundance of these transcripts was considerably higher, supporting that this cultivar has an efficient mechanism of restriction to Na^+ uptake, which contributes to minimize the damage caused by this ion in growth and efficiency photosynthetic, culminating in a better performance to salinity (Baghour et al., 2019; Miranda et al., 2017; Zhang et al., 2018). Although the expression of *OsSOS3* is higher only at 24 h, there is no difference between control and salt treatments at 12 and 48 h. However, the maintenance of basal levels of *OsSOS3* associated with the higher expression of *OsSOS1* and *OsSOS2* at 12 h in the SF is consistent with their role Na^+ sensor and antiport activity (Ji et al., 2013). On the other hand, the lower expression *OsSOS3* that occurs in the ES cultivar may be crucial to salt sensibility, as observed in Arabidopsis and brassica (Nutan et al., 2017; Ye et al., 2013)

Concerning the NHX genes, six members of the NHX family have

already been identified in the rice genome (Fu et al., 2018; Zhang et al., 2018), but in the cultivars analyzed under experimental conditions, only *OsNHX1*, *OsNHX2*, *OsNHX3*, and *OsNHX5* genes were detected. The abundance of *OsNHX1* and *OsNHX2* transcripts was increased more in SF than in ES under salt stress (Fig. 7d–g). Similarly, expression peaks of *OsNHX3* occurred 24 h after the onset of salt stress in the SF cultivar. Despite the *gene* expression stimulation of *OsNHX5*, this seems not to be involved with differential tolerance to salinity of the ES and SF cultivars since there is not a clear pattern in its expression over time. On the other hand, our findings suggest that there was compartmentalization of Na^+ in the vacuoles (Fig. 6) associated with the higher expression of *OsNHX1* and *OsNHX2* at all times evaluated, contributing to maintaining a high K^+/Na^+ ratio in the cytosol and tolerance to saline stress in SF cultivar. Otherwise, there is no clear expression pattern of NHX genes amount in ES over time; for instance, *OsNHX1* was higher only at 48 h, and *OsNHX2* was slightly increased only at 24 h, which was not capable of dealing with all Na^+ content presented earlier. In agreement, other authors also showed that transgenic plants overexpressing NHX family members presented beneficial physiological changes, such as maintenance of redox homeostasis, increased chlorophyll, and proline contents, which contribute to an increased tolerance to salt stress compared to wild plants (Baghour et al., 2019; Huang et al., 2018; Mushke et al., 2019), including high K^+/Na^+ ratio (Wang et al., 2019). Collectively, the data presented here show that the most salt-tolerant cultivar (SF) modulates integrated responses to NaCl stress, which prevents the harmful effects of salinity in growth and photosynthetic capacity. In this way, all work contributes to understanding the complex accumulation mechanisms of sodium and their impacts on the photosynthetic system. We provided a suitable discussion of the relationship of attributes concerning structural, functional, biochemical, and molecular adjustments that lead to salt tolerance differences in rice genotypes. On this hand, the future perspective is to combine our results with omics data and mathematical models (integrated network analysis) to integrate and expand the knowledge of complex plant metabolism (Jamil et al., 2020).

5. Conclusion

The study confirmed contrasting salt stress tolerance between ES and SF rice cultivars observed in previous experiments to choose cultivars. The salt stress tolerance was related to ionic homeostasis and photosynthetic efficiency maintenance. The salt-tolerant cultivar (São Francisco) has more efficient transcriptional and functional regulatory mechanisms than the salt-sensitive cultivar (BRS Esmeralda), based on their capacity to minimize the toxicity of Na^+ in the cytosol, the harmful effects in the gas exchanges, energy capture, electron transport, and integrity of chloroplasts. These adjustments allowed the SF cultivar to grow better in saline environments than the ES cultivar, minimizing the damage imposed by this salt stress.

Author agreement

All authors have read and approved the manuscript.

CRediT authorship contribution statement

Cibelle Gomes Gadelha: Conceptualization, Methodology, Formal analysis, Investigation, Data curation, Writing - original draft, Visualization. **Ítalo Antônio Cotta Coutinho:** Formal analysis, Validation, Writing - review & editing. **Sergimar Kennedy de Paiva Pinheiro:** Formal analysis, Data curation. **Emilio de Castro Miguel:** Validation, Writing - review & editing. **Humberto Henrique de Carvalho:** Validation, Writing - review & editing. **Lineker de Sousa Lopes:** Data curation, Validation, Writing - review & editing. **Enéas Gomes-Filho:** Validation, Resources, Supervision, Funding acquisition.

Declaration of Competing Interest

The authors declare that they have no conflict of interest.

Acknowledgments

This work was supported by the Coordenação de Aperfeiçoamento de Pessoal de Nível Superior (CAPES), Conselho Nacional de Desenvolvimento Científico e Tecnológico (CNPq), Instituto Nacional de Ciência e Tecnologia em Salinidade (INCTSal / CNPq, Brazil), and Fundação Cearense de Apoio ao Desenvolvimento Científico e Tecnológico (FUNCAP). The authors thank Central Analítica at Federal University of Ceará for assistance with the electron microscopy analyses (Central Analítica-UFC/CT-INFRA/MCTI-SISANO/Pró-Equipamentos CAPES) and Instituto Agronômico de Pernambuco (IPA) for providing rice seeds. Fellowship granted by CNPq to EGF and CAPES to CGG and LSL are gratefully acknowledged.

Appendix A. Supplementary data

Supplementary material related to this article can be found, in the online version, at doi:https://doi.org/10.1016/j.envexpbot.2021.104654.

References

Araújo, G.S., Miranda, R.S., Mesquita, R.O., Paula, S.O., Prisco, J.T., Gomes-Filho, E., 2018. Nitrogen assimilation pathways and ionic homeostasis are crucial for photosynthetic apparatus efficiency in salt-tolerant sunflower genotypes. Plant Growth Regul. 86, 375–388. https://doi.org/10.1007/s10725-018-0436-y.

Araújo, G.S., Paula-Marinho, S.O., Pinheiro, S.K.P., Miguel, E.C., Lopes, L.S., Marques, E. C., Carvalho, H.H., Gomes-Filho, E., 2021. H_2O_2 priming promotes salt tolerance in maize by protecting chloroplasts ultrastructure and primary metabolites modulation. Plant Sci. 303, 110774 https://doi.org/10.1016/j.plantsci.2020.110774.

Ashraf, M., Harris, P.J.C., 2013. Photosynthesis under stressful environments: an overview. Photosynthetica 51, 163–190. https://doi.org/10.1007/s11099-013-0021-6.

Assaha, D.V.M., Ueda, A., Saneoka, H., Al-Yahyai, R., Yaish, M.W., 2017. The role of Na^+ and K^+ transporters in salt stress adaptation in glycophytes. Front. Physiol. 8 https://doi.org/10.3389/fphys.2017.00509.

Baghour, M., Gálvez, F.J., Sánchez, M.E., Aranda, M.N., Venema, K., Rodríguez-Rosales, M.P., 2019. Overexpression of LeNHX2 and SlSOS2 increases salt tolerance and fruit production in double transgenic tomato plants. Plant Physiol. Biochem. 135, 77–86. https://doi.org/10.1016/j.plaphy.2018.11.028.

Barnes, J.D., Balaguer, L., Manrique, E., Elvira, S., Davison, A.W., 1992. A reappraisal of the use of DMSO for the extraction and determination of chlorophylls a and b in lichens and higher plants. Environ. Exp. Bot. 32, 85–100. https://doi.org/10.1016/0098-8472(92)90034-Y.

Bejaoui, F., Salas, J.J., Nouairi, I., Smaoui, A., Abdelly, C., Martínez-Force, E., Youssef, N. Ben, 2016. Changes in chloroplast lipid contents and chloroplast ultrastructure in Sulla carnosa and Sulla coronaria leaves under salt stress. J. Plant Physiol. 198, 32–38. https://doi.org/10.1016/j.jplph.2016.03.018.

Bertazzini, M., Sacchi, G.A., Forlani, G., 2018. A differential tolerance to mild salt stress conditions among six Italian rice genotypes does not rely on Na^+ exclusion from shoots. J. Plant Physiol. 226, 145–153. https://doi.org/10.1016/j.jplph.2018.04.011.

Castro, A.P., Morais, O.P., Breseghello, F., Lobo, V.Lda S., Guimarães, C.M., Bassinello, P. Z., Colombari Filho, J.M., Santiago, C.M., Furtini, I.V., Torga, P.P., Utumi, M.M., Pereira, J.A., Cordeiro, A.C.C., Azevedo, R., Sousa, N.R.G., Soares, A.A., Radmann, V., Peters, V.J., 2014. BRS Esmeralda: upland rice cultivar with high productivity and greater drought tolerance. Embrapa Arroz e Feijão-Comunicado Técnico. Embrapa Arroz e Feijão, Santo Antônio de Goiás.

Çelik, Ö., Meriç, S., Ayan, A., Atak, Ç., 2019. Epigenetic analysis of WRKY transcription factor genes in salt stressed rice (*Oryza sativa* L.) plants. Environ. Exp. Bot. 159, 121–131. https://doi.org/10.1016/j.envexpbot.2018.12.015.

Chakraborty, K., Chattaopadhyay, K., Nayak, L., Ray, S., Yeasmin, L., Jena, P., Gupta, S., Mohanty, S.K., Swain, P., Sarkar, R.K., 2019. Ionic selectivity and coordinated transport of Na^+ and K^+ in flag leaves render differential salt tolerance in rice at the reproductive stage. Planta 250, 1637–1653. https://doi.org/10.1007/s00425-019-03253-9.

Chang, J., Cheong, B.E., Natera, S., Roessner, U., 2019. Morphological and metabolic responses to salt stress of rice (*Oryza sativa* L.) cultivars which differ in salinity tolerance. Plant Physiol. Biochem. 144, 427–435. https://doi.org/10.1016/j.plaphy.2019.10.017.

Cheng, D., Wu, G., Zheng, Y., 2015. Positive correlation between potassium uptake and salt tolerance in wheat. Photosynthetica 53, 447–454. https://doi.org/10.1007/s11099-015-0124-3.

Chutimanukul, P., Kositsup, B., Plaimas, K., Buaboocha, T., Siangliw, M., Toojinda, T., Comai, L., Chadchawan, S., 2018. Photosynthetic responses and identification of salt tolerance genes in a chromosome segment substitution line of 'Khao dawk Mali 105' rice. Environ. Exp. Bot. 155, 497–508. https://doi.org/10.1016/j.envexpbot.2018.07.019.

Clark, R.B., 1975. Characterization of phosphatase of intact maize roots. J. Agric. Food Chem. 23, 458–460. https://doi.org/10.1021/jf60199a002.

Cuin, T.A., Bose, J., Stefano, G., Jha, D., Tester, M., Mancuso, S., Shabala, S., 2011. Assessing the role of root plasma membrane and tonoplast Na^+ /H^+ exchangers in salinity tolerance in wheat: in planta quantification methods. Plant Cell Environ. 34, 947–961. https://doi.org/10.1111/j.1365-3040.2011.02296.x.

Du, Q., Zhao, Xhua, Xia, L., Jiang, Cji, Wang, Xguang, Han, Y., Wang, J., Yu, Hqiu, 2019. Effects of potassium deficiency on photosynthesis, chloroplast ultrastructure, ROS, and antioxidant activities in maize (Zea mays L.). J. Integr. Agric. 18, 395–406. https://doi.org/10.1016/S2095-3119(18)61953-7.

EMBRAPA, 2013. Catalog of rice cultivars. Embrapa Arroz e Feijão. Santo Antônio de Goiás.

Evert, R.F., 2006. Esau's Plant Anatomy, Esau's Plant Anatomy: Meristems, Cells, and Tissues of the Plant Body: Their Structure, Function, and Development, 3rd ed. John Wiley & Sons, Inc., Hoboken, NJ, USA https://doi.org/10.1002/0470047380.

FAO, 2019. Statistics - Food and Agriculture Organization of the United Nations [WWW Document]. http://www.fao.org/statistics/en (Accessed 12.2.19).

Frukh, A., Siddiqi, T.O., Khan, M.I.R., Ahmad, A., 2020. Modulation in growth, biochemical attributes and proteome profile of rice cultivars under salt stress. Plant Physiol. Biochem. 146, 55–70. https://doi.org/10.1016/j.plaphy.2019.11.011.

Fu, L., Shen, Q., Kuang, L., Yu, J., Wu, D., Zhang, G., 2018. Metabolite profiling and gene expression of Na/K transporter analyses reveal mechanisms of the difference in salt tolerance between barley and rice. Plant Physiol. Biochem. 130, 248–257. https://doi.org/10.1016/j.plaphy.2018.07.013.

Gadelha, C.G., Miranda, R.S., Alencar, N.L.M., Costa, J.H., Prisco, J.T., Gomes-Filho, E., 2017. Exogenous nitric oxide improves salt tolerance during establishment of *Jatropha curcas* seedlings by ameliorating oxidative damage and toxic ion accumulation. J. Plant Physiol. 212, 69–79. https://doi.org/10.1016/j.jplph.2017.02.005.

Gerona, M.E.B., Deocampo, M.P., Egdane, J.A., Ismail, A.M., Dionisio-Sese, M.L., 2019. Physiological responses of contrasting rice genotypes to salt stress at reproductive stage. Rice Sci. 26, 207–219. https://doi.org/10.1016/j.rsci.2019.05.001.

Goussi, R., Manaa, A., Derbali, W., Cantamessa, S., Abdelly, C., Barbato, R., 2018. Comparative analysis of salt stress, duration and intensity, on the chloroplast ultrastructure and photosynthetic apparatus in *Thellungiella salsuginea*. J. Photochem. Photobiol. B Biol. 183, 275–287. https://doi.org/10.1016/j.jphotobiol.2018.04.047.

Gupta, P., Yadav, C., Singla-Pareek, S.L., Pareek, A., 2018. Recent advancements in developing salinity tolerant rice. Advances in Rice Research for Abiotic Stress Tolerance. Elsevier, pp. 87–112. https://doi.org/10.1016/B978-0-12-814332-2.00005-8.

Hasegawa, P.M., 2013. Sodium (Na^+) homeostasis and salt tolerance of plants. Environ. Exp. Bot. 92, 19–31. https://doi.org/10.1016/j.envexpbot.2013.03.001.

Hoang, T., Tran, T., Nguyen, T., Williams, B., Wurm, P., Bellairs, S., Mundree, S., 2016. Improvement of salinity stress tolerance in rice: challenges and opportunities. Agronomy 6, 54. https://doi.org/10.3390/agronomy6040054.

Huang, Y., Zhang, X., Li, Y., Ding, J., Du, H., Zhao, Z., Zhou, L., Liu, C., Gao, S., Cao, M., Lu, Y., Zhang, S., 2018. Overexpression of the Suaeda salsa SsNHX1 gene confers enhanced salt and drought tolerance to transgenic Zea mays. J. Integr. Agric. 17, 2612–2623. https://doi.org/10.1016/S2095-3119(18)61998-7.

Islam, F., Wang, J., Farooq, M.A., Yang, C., Jan, M., Mwamba, T.M., Hannan, F., Xu, L., Zhou, W., 2019. Responses and tolerance to salt stress. Advances in Rice Research for Abiotic Stress Tolerance. Elsevier, pp. 791–819. https://doi.org/10.1016/B978-0-12-814332-2.00040-X.

Jamil, I.N., Remali, J., Azizan, K.A., Nor Muhammad, N.A., Arita, M., Goh, H.-H., Aizat, W.M., 2020. Systematic multi-omics integration (MOI) approach in plant systems biology. Front. Plant Sci. 0, 944. https://doi.org/10.3389/FPLS.2020.00944.

Ji, H., Pardo, J.M., Batelli, G., Van Oosten, M.J., Bressan, R.A., Li, X., 2013. The salt overly sensitive (SOS) pathway: established and emerging roles. Mol. Plant 6, 275–286. https://doi.org/10.1093/mp/sst017.

Johansen, D.A., 1940. Plant Microtechnique. McGraw-Hill Publ. Co., Ltd., Aldwych House, London, W.C.2, New York and London.

Kandula, V., Pudutha, A., Kumari, P.H., Kumar, S.A., Kavi Kishor, P.B., Anupalli, R.R., 2019. Overexpression of Sorghum plasma membrane-bound Na+/H+ antiporter-like protein (SbNHXLP) enhances salt tolerance in transgenic groundnut (*Arachis hypogaea* L.). Plant Cell Tissue Organ Cult. 138, 325–337. https://doi.org/10.1007/s11240-019-01628-0.

Keisham, M., Mukherjee, S., Bhatla, S.C., 2018. Mechanisms of sodium transport in plants—progresses and challenges. Int. J. Mol. Sci. 19 https://doi.org/10.3390/ijms19030647.

Kellogg, E.A., 2015. Description of the family, vegetative morphology and anatomy. Flowering Plants. Monocots. Springer International Publishing, Cham, pp. 3–23. https://doi.org/10.1007/978-3-319-15332-2_1.

Khan, M.S., Ahmad, D., Khan, M.A., 2015. Trends in genetic engineering of plants with (Na+/H+) antiporters for salt stress tolerance. Biotechnol. Biotechnol. Equip. 29, 815–825. https://doi.org/10.1080/13102818.2015.1060868.

Krishnamurthy, P., Vishal, B., Khoo, K., Rajappa, S., Loh, C.S., Kumar, P.P., 2019. Expression of AoNHX1 increases salt tolerance of rice and Arabidopsis, and bHLH transcription factors regulate AtNHX1 and AtNHX6 in Arabidopsis. Plant Cell Rep. 38, 1299–1315. https://doi.org/10.1007/s00299-019-02450-w.

Lamy, C.M., Chatton, J.Y., 2011. Optical probing of sodium dynamics in neurons and astrocytes. NeuroImage 58, 572–578. https://doi.org/10.1016/j.neuroimage.2011.06.074.

Liu, J., Shabala, S., Shabala, L., Zhou, M., Meinke, H., Venkataraman, G., Chen, Z., Zeng, F., Zhao, Q., 2019. Tissue-specific regulation of Na^+ and K^+ transporters explains genotypic differences in salinity stress tolerance in rice. Front. Plant Sci. 10, 1–15. https://doi.org/10.3389/fpls.2019.01361.

Livak, K.J., Schmittgen, T.D., 2001. Analysis of relative gene expression data using real-time quantitative PCR and the $2^{-\Delta\Delta C}_T$ method. Methods 25, 402–408. https://doi.org/10.1006/meth.2001.1262.

Lopes, L.S., Carvalho, H.H., Miranda, R.S., Gallão, M.I., Gomes-Filho, E., 2020. The influence of dissolved oxygen around rice roots on salt tolerance during pre-tillering and tillering phases. Environ. Exp. Bot. 178, 104169 https://doi.org/10.1016/j.envexpbot.2020.104169.

Mahlooji, M., Seyed Sharifi, R., Razmjoo, J., Sabzalian, M.R., Sedghi, M., 2018. Effect of salt stress on photosynthesis and physiological parameters of three contrasting barley genotypes. Photosynthetica 56, 549–556. https://doi.org/10.1007/s11099-017-0699-y.

Majeed, A., Muhammad, Z., 2019. Salinity: a major agricultural problem-causes, impacts on crop productivity and management strategies. Plant Abiotic Stress Tolerance: Agronomic, Molecular and Biotechnological Approaches. Springer International Publishing, pp. 83–99. https://doi.org/10.1007/978-3-030-06118-0_3.

Malavolta, E., Vitti, G.C., de Oliveira, S.A., 1989. Evaluation of the nutritional state of plants: principles and applications. Associacao Brasileira para Pesquisa da Potassa e do Fosfato. Associação Brasileira para Pesquisa da Potasse e do Fosfato, Piracicaba.

Mancarella, S., Orsini, F., van Oosten, M.J., Sanoubar, R., Stanghellini, C., Kondo, S., Gianquinto, G., Maggio, A., 2016. Leaf sodium accumulation facilitates salt stress adaptation and preserves photosystem functionality in salt stressed *Ocimum basilicum*. Environ. Exp. Bot. 130, 162–173. https://doi.org/10.1016/j.envexpbot.2016.06.004.

Mantri, N., Patade, V., Penna, S., Ford, R., Pang, E., 2012. Abiotic stress responses in plants: present and future. Abiotic Stress Responses in Plants. Springer, New York, New York, NY, pp. 1–19. https://doi.org/10.1007/978-1-4614-0634-1_1.

Marriboina, S., Sengupta, D., Kumar, S., Reddy, A.R., 2017. Physiological and molecular insights into the high salinity tolerance of *Pongamia pinnata* L. pierre, a potential biofuel tree species. Plant Sci. 258, 102–111. https://doi.org/10.1016/j.plantsci.2017.02.008.

Matschi, S., Vasquez, M.F., Bourgault, R., Steinbach, P., Chamness, J., Kaczmar, N., Gore, M.A., Molina, I., Smith, L.G., 2020. Structure-function analysis of the maize bulliform cell cuticle and its potential role in dehydration and leaf rolling. Plant Direct 4, e00282. https://doi.org/10.1002/pld3.282.

McVeigh, I., 1935. A simple method for bleaching leaves. Stain Technol. 10, 33–34. https://doi.org/10.3109/10520293509116004.

Miranda, R.S., Gomes-Filho, E., Prisco, J.T., Alvarez-Pizarro, J.C., 2016. Ammonium improves tolerance to salinity stress in *Sorghum bicolor* plants. Plant Growth Regul. 78, 121–131. https://doi.org/10.1007/s10725-015-0079-1.

Miranda, R.S., Mesquita, R.O., Costa, J.H., Alvarez-Pizarro, J.C., Prisco, J.T., Gomes-Filho, E., 2017. Integrative control between proton pumps and SOS1 antiporters in roots is crucial for maintaining Low Na+ accumulation and salt tolerance in ammonium-supplied *Sorghum bicolor*. Plant Cell Physiol. 58, 522–536. https://doi.org/10.1093/pcp/pcw231.

Mirdar Mansuri, R., Shobbar, Z.S., Babaeian Jelodar, N., Ghaffari, M.R., Nematzadeh, G. A., Asari, S., 2019. Dissecting molecular mechanisms underlying salt tolerance in rice: a comparative transcriptional profiling of the contrasting genotypes. Rice 12. https://doi.org/10.1186/s12284-019-0273-2.

Mushke, R., Yarra, R., Kirti, P.B., 2019. Improved salinity tolerance and growth performance in transgenic sunflower plants via ectopic expression of a wheat antiporter gene (TaNHX2). Mol. Biol. Rep. 46, 5941–5953. https://doi.org/10.1007/s11033-019-05028-7.

Najar, R., Aydi, S., Sassi-Aydi, S., Zarai, A., Abdelly, C., 2019. Effect of salt stress on photosynthesis and chlorophyll fluorescence in *Medicago truncatula*. Plant Biosyst. - Int. J. Deal. With All Asp. Plant Biol. 153, 88–97. https://doi.org/10.1080/11263504.2018.1461701.

Negrão, S., Schmöckel, S.M., Tester, M., 2017. Evaluating physiological responses of plants to salinity stress. Ann. Bot. 119, 1–11. https://doi.org/10.1093/aob/mcw191.

Nie, W., Gong, B., Chen, Y., Wang, J., Wei, M., Shi, Q., 2018. Photosynthetic capacity, ion homeostasis and reactive oxygen metabolism were involved in exogenous salicylic acid increasing cucumber seedlings tolerance to alkaline stress. Sci. Hortic. 235, 413–423. https://doi.org/10.1016/j.scienta.2018.03.011.

Nowicka, B., Ciura, J., Szymańska, R., Kruk, J., 2018. Improving photosynthesis, plant productivity and abiotic stress tolerance – current trends and future perspectives. J. Plant Physiol. 231, 415–433. https://doi.org/10.1016/j.jplph.2018.10.022.

Nutan, K.K., Kumar, G., Singla-Pareek, S.L., Pareek, A., 2017. A salt overly sensitive pathway member from Brassica juncea BjSOS3 can functionally complement ΔAtsos3 in Arabidopsis. Curr. Genomics 19. https://doi.org/10.2174/1389202918666170228133621.

Pan, Y.Q., Guo, H., Wang, S.M., Zhao, B., Zhang, J.L., Ma, Q., Yin, H.J., Bao, A.K., 2016. The photosynthesis, Na^+/K^+ homeostasis and osmotic adjustment of atriplex canescens in response to salinity. Front. Plant Sci. 7, 1–14. https://doi.org/10.3389/fpls.2016.00848.

Pandolfi, C., Mancuso, S., Shabala, S., 2012. Physiology of acclimation to salinity stress in pea (*Pisum sativum*). Environ. Exp. Bot. 84, 44–51. https://doi.org/10.1016/j.envexpbot.2012.04.015.

Passricha, N., Saifi, S.K., Kharb, P., Tuteja, N., 2019. Marker-free transgenic rice plant overexpressing pea LecRLK imparts salinity tolerance by inhibiting sodium

accumulation. Plant Mol. Biol. 99, 265–281. https://doi.org/10.1007/s11103-018-0816-8.

Peres, A.R., Rodrigues, R.A.F., Portugal, J.R., Arf, O., Gonzaga, A.R., Meirelles, F.C., Garcia, N.F.S., Corsini, D.C.D.C., Takasu, A.T., 2018. Effect of irrigatation, rainfed conditions and nitrogen sources on newly released upland rice cultivar (BRS Esmeralda) with greater tolerance to drought stress. Aust. J. Crop Sci. 12, 1072–1081. https://doi.org/10.21475/ajcs.18.12.07.PNE889.

Prisco, J.T., Gomes-Filho, E., Miranda, R.S., 2016. Physiology and biochemistry of plants growing under salt stress. Manejo da salinidade na agricultura: Estudos básicos e aplicados, pp. 163–180.

Qu, C., Liu, C., Gong, X., Li, C., Hong, M., Wang, L., Hong, F., 2012. Impairment of maize seedling photosynthesis caused by a combination of potassium deficiency and salt stress. Environ. Exp. Bot. 75, 134–141. https://doi.org/10.1016/j.envexpbot.2011.08.019.

Radanielson, A.M., Angeles, O., Li, T., Ismail, A.M., Gaydon, D.S., 2018. Describing the physiological responses of different rice genotypes to salt stress using sigmoid and piecewise linear functions. Field Crops Res. 220, 46–56. https://doi.org/10.1016/j.fcr.2017.05.001.

Riaz, M., Arif, M.S., Ashraf, M.A., Mahmood, R., Yasmeen, T., Shakoor, M.B., Shahzad, S. M., Ali, M., Saleem, I., Arif, M., Fahad, S., 2019. A comprehensive review on rice responses and tolerance to salt stress. Advances in Rice Research for Abiotic Stress Tolerance. Elsevier, pp. 133–158. https://doi.org/10.1016/B978-0-12-814332-2.00007-1.

Roder, P., Hille, C., 2014. ANG-2 for quantitative Na+ determination in living cells by time-resolved fluorescence microscopy. Photochem. Photobiol. Sci. 13, 1699–1710. https://doi.org/10.1039/c4pp00061g.

Shahzad, B., Fahad, S., Tanveer, M., Saud, S., Khan, I.A., 2019. Plant responses and tolerance to salt stress. Approaches for Enhancing Abiotic Stress Tolerance in Plants. CRC Press, Boca Raton, FL, pp. 61–78. https://doi.org/10.1201/9781351104722-3. CRC Press, Taylor & Francis Group, 2019.

Silva, M.M.B., Santana, A.S.C.O., Pimentel, R.M.M., Silva, F.C.L., Randau, K.P., Soares, L. A.L., 2013. Anatomy of leaf and stem of *Erythrina velutina*. Braz. J. Pharmacogn. 23, 200–206. https://doi.org/10.1590/S0102-695X2013005000013.

Singh, A., Sengar, R.S., 2014. Salinity stress in rice: an overview. Plant Arch. 14, 643–648.

Singh, D., Singh, B., Mishra, S., Singh, A.K., Singh, N.K., 2019. Candidate gene based association analysis of salt tolerance in traditional and improved varieties of rice (*Oryza sativa* L.). J. Plant Biochem. Biotechnol. 28, 76–83. https://doi.org/10.1007/s13562-018-0464-8.

Tang, Y.Y., Yuan, Y.H., Shu, S., Guo, S.R., 2018. Regulatory mechanism of NaCl stress on photosynthesis and antioxidant capacity mediated by transglutaminase in cucumber (*Cucumis sativus* L.) seedlings. Sci. Hortic. 235, 294–306. https://doi.org/10.1016/j.scienta.2018.02.045.

Tsai, Y.C., Chen, K.C., Cheng, T.S., Lee, C., Lin, S.H., Tung, C.W., 2019. Chlorophyll fluorescence analysis in diverse rice varieties reveals the positive correlation between the seedlings salt tolerance and photosynthetic efficiency. BMC Plant Biol. 19, 403. https://doi.org/10.1186/s12870-019-1983-8.

Tucker, S.C., 1957. Ontogeny of the etiolated seedling mesocotyl of *Zea mays*. Bot. Gaz. 118, 160–174. https://doi.org/10.1086/335940.

Wang, J., Qiu, N., Wang, P., Zhang, W., Yang, X., Chen, M., Wang, B., Sun, J., 2019. Na^+ compartmentation strategy of *Chinese cabbage* in response to salt stress. Plant Physiol. Biochem. 140, 151–157. https://doi.org/10.1016/j.plaphy.2019.05.001.

Wellburn, A.R., 1994. The spectral determination of chlorophylls a and b, as well as total carotenoids, using various solvents with spectrophotometers of different resolution. J. Plant Physiol. 144, 307–313. https://doi.org/10.1016/S0176-1617(11)81192-2.

Wu, H., 2018. Plant salt tolerance and Na^+ sensing and transport. Crop J. 6, 215–225. https://doi.org/10.1016/j.cj.2018.01.003.

Yamaguchi, T., Hamamoto, S., Uozumi, N., 2013. Sodium transport system in plant cells. Front. Plant Sci. 4, 1–7. https://doi.org/10.3389/fpls.2013.00410.

Yamane, K., Mitsuya, S., Taniguchi, M., Miyake, H., 2012. Salt-induced chloroplast protrusion is the process of exclusion of ribulose-1,5-bisphosphate carboxylase/oxygenase from chloroplasts into cytoplasm in leaves of rice. Plant Cell Environ. 35, 1663–1671. https://doi.org/10.1111/j.1365-3040.2012.02516.x.

Ye, J., Zhang, W., Guo, Y., 2013. Arabidopsis SOS3 plays an important role in salt tolerance by mediating calcium-dependent microfilament reorganization. Plant Cell Rep. 32, 139–148. https://doi.org/10.1007/s00299-012-1348-3.

Zhang, Y., Fang, J., Wu, X., Dong, L., 2018. Na^+ /K^+ balance and transport regulatory mechanisms in weedy and cultivated rice (*Oryza sativa* L.) under salt stress. BMC Plant Biol. 18, 1–14. https://doi.org/10.1186/s12870-018-1586-9.

Zhu, Yfang, Wu, Yxia, Hu, Y., Jia, Xmei, Zhao, T., Cheng, L., Wang, Yxiu, 2019. Tolerance of two apple rootstocks to short-term salt stress: focus on chlorophyll degradation, photosynthesis, hormone and leaf ultrastructures. Acta Physiol. Plant. 41 https://doi.org/10.1007/s11738-019-2877-y.